

ABSTRACT

BRYANT, SHANTE SHERELLE. The Influence of Genetic Background on Experimentally-Induced Colitis in Murine Models of Inflammatory Bowel Disease (Under the direction of Dr. David Threadgill, Dr. Anthony Blikslager, and Dr. Reade Roberts).

Inflammatory Bowel Disease (IBD) is comprised of two main conditions, ulcerative colitis (UC) and Crohn's disease (CD), which represent a heterogeneous group of diseases that are characterized by chronic intestinal inflammation. The pathogenesis of IBD remains poorly understood but clinical evidence supports that the aberrant inflammatory response results from complex interactions between genetic and environmental factors. Perturbations in the normal tolerogenic immune response to resident luminal bacteria is a key feature that is present in patients affected by IBD. The importance of the intestinal microbiome in the etiology of IBD has initiated interest in the role played by intestinal epithelial cells and their ability to maintain the structure and function of the intestinal barrier. Alterations in intestinal permeability have been documented in both UC and CD patients and has been recorded in mouse models of intestinal inflammation.

Several animal models of IBD exist, and differential susceptibility to experimentally-induced intestinal inflammation among various inbred mouse strains is well documented. Two strains of particular interest, BALB/c and C57BL/6, have opposite responses to the commonly used DSS and TNBS-induced colitis models.

We utilized the distinct responses of these strains to help characterize these models in terms of intestinal barrier function and for identification of genetic variants that potentially influence disease severity. We found a significant difference in intestinal barrier permeability for the DSS model in susceptible C57BL/6 mice. This defect in barrier regulation was apparent for up to two weeks after DSS administration even when overt signs of inflammation had dissipated.

In contrast, no changes in epithelial barrier function were found in the TNBS-model. Furthermore, QTL mapping in a F2 population generated from parental BALB/c and C57BL/6 mice revealed several suggestive QTL that were exclusive to each model. We discuss the limitations of our QTL analysis and approaches to increase our ability to detect significant QTL. A combinatorial method using gene expression and mapping data is also proposed as a way to reduce the number of candidate genes that may be identified in our refined mapping analysis.

Genes that are located inside significant QTL regions, are differential expressed, and involved in biological pathways related to intestinal barrier maintenance are of the highest priority as they may provide insights into the mechanisms underlying the observations of alterations in intestinal permeability outlined in chapter 2 of this dissertation. Additionally, proposed 16S phylogenetic analysis of samples collected from parental strains and F2CB mice could prove useful for describing host-microbe interactions and pinpointing bacterial species that affect disease severity in human IBD.

© Copyright 2019 by Shante Sherelle Bryant

All Rights Reserved

The Influence of Genetic Background on Experimentally-Induced Colitis in Murine Models of
Inflammatory Bowel Disease

by
Shante Sherelle Bryant

A dissertation submitted to the Graduate Faculty of
North Carolina State University
in partial fulfillment of the
requirements for the degree of
Doctor of Philosophy

Genetics

Raleigh, North Carolina
2019

APPROVED BY:

Dr. David Threadgill
Committee Co-Chair

Dr. Anthony Blikslager
Committee Co-Chair

Dr. Reade Roberts
Committee Co-Chair

Dr. Eric Stone

DEDICATION

I dedicate this dissertation to my parents, my husband, and my closest friends. Without your constant support and encouragement, none of this would have been possible. Thanks for always believing in me even when I didn't believe in myself. To my sister, Hailey, remember that if I can do this, you can accomplish anything in this world.

BIOGRAPHY

Shante Sherelle Bryant was born in Wilmington, NC on July 9, 1989, to Debra Jacobs and James Bryant. She grew up in a small town called Buckhead, home of the Waccamaw Siouan tribe, and attended East Columbus High School in Lake Waccamaw, NC. After graduation, she attended North Carolina State University where she majored in Biochemistry with a minor in Genetics. During her time as an undergraduate at NCSU, she met her husband and a group of very special friends that have been by her side since her sophomore year. She also had the opportunity to work in the lab of Margaret Daub studying interactions between fungal pathogens and their plant hosts. After earning her bachelor's degree, she remained at NCSU to pursue a graduate degree in Genetics. She joined the lab of Dr. David Threadgill and was later adopted by Dr. Anthony Blikslager. She has been extremely grateful for the chance to be co-mentored by two brilliant scientists during her time as a PhD student.

ACKNOWLEDGMENTS

I'd like to extend my first thank you to my advisors, David Threadgill and Anthony Blikslager. Without your support and guidance, I never would have made it through this experience. I know it took much longer than you both expected, but thanks for never giving up on me. Special thanks to both past and present members of the Threadgill and Blikslager labs for helping me to navigate my way through my research projects. Threadgill lab: Rachel Lynch, Bill Barrington, Andrew Hillhouse, Tiffany Garbutt, Dona Kanavy, and Anna Salvador. Blikslager Lab: Younggeon Jin, Liara Gonzales, Tiffany Pridgen, Zachary Slifer, Leandi Krüger, and Amanda Ziegler. Major thanks to Dr. Reade Roberts for stepping in at the last minute to serve on my committee and Dr. Eric Stone for sticking with me from halfway across the globe.

I'd like to thank my husband, Adam Berry, for his continued encouragement even after witnessing me cycle through phases of confidence and utter fear while working on this degree. Thanks to my squad of friends: John Craig, Taylen Harp, Whitney King, Ashely Jones, Candice Bruinton, Evelyn Miller, Elise Brace, Aisha Chavis, and Chantell Felder for being such amazing motivators and great inspirations. Most of you started grad school after I did but still managed to finish before me. I'm looking forward to joining you on the other side. Thank you for surprising me with tickets to RuPaul's DragCon as an early graduation gift last year. I'm sorry that I cussed you all out because I don't like surprises. The experience was amazing, and the queens gave me life. I was encouraged to push even harder to graduate, so I wouldn't let you all down and waste the money you spent on my tickets. But in all seriousness, you mean the world to me and I wouldn't be writing this dissertation if it wasn't for your continued love and support.

Finally, thank you to my parents for being there for me no matter what. For encouraging me to never give up and keep pushing to the end. I hope I've made you proud.

TABLE OF CONTENTS

LIST OF TABLES	vi
LIST OF FIGURES	vii
Chapter 1: Inflammatory Bowel Disease: Mechanisms and Models	1
Introduction.....	2
Gastrointestinal Immune System Overview	2
Role of the Epithelial Barrier in Inflammatory Bowel Disease	7
Genetic Contributions to Inflammatory Bowel Disease Pathogenesis	10
Animal Models of Inflammatory Bowel Disease	13
Relevance of this Research Project.....	18
References.....	27
Chapter 2: Effect of Genetic Background on Intestinal Permeability in DSS and TNBS-Induced Colitis Models of Inflammatory Bowel Disease.....	38
Abstract	39
Introduction.....	41
Materials/Methods	43
Results.....	46
Discussion	49
References.....	61
Chapter 3: Genetic Analysis of DSS and TNBS-Induced Colitis on BALB/c and C57BL/6 Backgrounds.....	64
Abstract	65
Introduction.....	66
Materials/Methods	68
Results.....	70
Discussion	71
References.....	81
Chapter 4: Future Directions and Conclusions.....	85
Research Summary	86
Future Directions/Follow-Up Studies	87
Conclusions.....	95
References.....	97

LIST OF TABLES

Table 1.1	Summary of significant CD, UC, and general IBD loci identified by GWAS.....	22
Table 2.1	Disease severity scoring system for DAI	60
Table 3.1	Summary of suggestive QTL locations from F2CB mapping.....	80

LIST OF FIGURES

Figure 1.1	Intestinal barrier function	20
Figure 1.2	Mouse models of IBD	21
Figure 2.1	Severity of DSS colitis	55
Figure 2.2	Distal colon histology in DSS colitis	56
Figure 2.3	Severity of TNBS colitis	57
Figure 2.4	Distal colon histology in TNBS colitis.....	58
Figure 2.5	Baseline epithelial permeability	59
Figure 2.6	<i>In vivo</i> paracellular permeability for DSS colitis model	59
Figure 2.7	<i>In vivo</i> paracellular permeability for TNBS colitis model	60
Figure 3.1	DAI and body weight correlation	77
Figure 3.2	Percent body weight comparisons for F2CB mice	77
Figure 3.3	F2CB DSS-day-5 QTL scan.....	78
Figure 3.4	F2CB DSS-day-8 QTL scan.....	79
Figure 3.5	F2CB TNBS QTL scan.....	80

CHAPTER 1

Inflammatory Bowel Disease: Mechanisms and Models

Introduction

Acute and chronic inflammatory diseases of the gastrointestinal tract result in significant morbidity and mortality with compromised quality of life and life expectancy (1,2). Notably, acute enteritis or diarrheal disease account for over 1 million deaths annually and is a leading cause of death worldwide (3) with higher mortality rates in developing countries (4).

Additionally, the number of people suffering from chronic inflammatory diseases of the intestine and chronic enteritis continues to rise (5,6). These chronic diseases have tremendously negative impacts on the health and well-being of affected individuals and inflict increased costs and burdens to healthcare systems globally. Understanding the conditions under which normal homeostasis is maintained and the underlying mechanisms of inflammatory disease is crucial for the development of effective treatment and prevention strategies for individuals predisposed to the development of gastrointestinal disease.

Gastrointestinal Immune System Overview

The gastrointestinal (GI) tract serves a multiplicity of roles in human physiology including the digestion and uptake of nutrients, along with maintaining immune homeostasis in order to protect the body from potentially harmful microorganisms while also inducing tolerance of commensal microbes and self-antigens. A unique immunological system exists within the GI tract that differs from the systemic immune system and provides immunological responses or tolerance to luminal bacteria and dietary antigens. Lymphoid cell aggregates, referred to as gut-associated lymphoid tissue (GALT), function as important induction sites for the mucosal immune response. In addition to GALT, there are abundant lymphoid cells in the intestinal lamina propria (LP) and epithelial lining that function as immune effector cells.

There are several phenotypically and functionally distinctive lymphocyte populations that constitute GALT. The architecture of the GALT is designed to limit and control immune response via separation of inductive and effector sites. Peyer's patches (PPs), isolated lymphoid follicles (ILFs), and mesenteric lymph nodes (MLNs) are representative inductive sites for immune responses in the intestinal mucosa. After exiting the inductive phase of the immune response, effector lymphocytes become scattered throughout the LP and epithelium of the mucosa (7,8).

PPs are secondary lymphoid tissue found in the submucosa of the small intestine. They are macroscopically visible domes with an organizational structure similar to that of lymph nodes and consist of a follicular B-cell zone with a germinal center surrounded by a T-cell zone area. PPs have high endothelial venules (HEVs) through which lymphocytes can enter from the blood and outgoing lymphatics that drain lymph away from the tissues. However, unlike lymph nodes, there are no incoming lymphatics that bring lymph into the PPs. This lack of afferent lymph vessels requires PPs to have a distinctive structure that enables uptake of antigens from the intestinal lumen. As a result, PPs are covered by a monolayer of epithelial cells known as the follicle-associated epithelium (FAE). The epithelial cells of this protective barrier are shorter and have less densely packed microvilli than the neighboring epithelium. Cells in the FAE include M-cells, which have a specialized structure and function for the uptake of macromolecules. These M-cells lack a brush border glycocalyx, as well as the typical mucus layer that coats their apical surface. As a result, microbes that inhabit the intestine are easily accessible by M-cells. They are able to enclose intestinal antigens in vesicles for transport from the lumen into the underlying subepithelial dome (SED). This region contains many immature dendritic cells (DCs) that process the antigens taken up by M-cells for presentation to lymphocytes (9).

Unlike PPs, ILFs are present in the LP of both the small and large intestine and are especially abundant in the distal ileum and colon where the number of intestinal bacteria is markedly increased. ILFs, like PPs, also have germinal centers and are covered by a distinctive FAE also containing M-cells. These ILFs are thought to originate from crypt patches which are small aggregates of T-cell progenitors in the crypt LP that are required for thymus-independent development of intraepithelial lymphocytes (IELs) (10).

Efferent lymphatics from both PPs and ILFs are drained into the MLNs. Although MLNs share the same basic structure as other lymph nodes of the body, there is evidence that the microenvironment within the MLNs differs from that in the peripheral lymph nodes (PLNs) (11,12). These lymphocytes undergo proliferation at a rate about four times higher than that of lymphocytes entering into the PLNs (12). Different proliferation rates of effector lymphocytes after entry into MLNs and PLNs are mediated by cytokines that are present in differing concentrations in the two types of lymph nodes.

After circulation in the blood, effector lymphocytes generated in the MLNs preferentially accumulate in MLNs and the mucosal sites drained by them (PPs, ILFs, and LP). They are primed for entry into the mucosa of the gut via upregulated expression of $\alpha 4\beta 7$ integrin (Peyer patches-specific homing receptor, LPAM1) and loss of L-selectin expression (CD62L) (13,14). These adhesion molecules normally direct lymphocytes to enter mucosal or peripheral tissues, respectively (15). Mucosal addressin cell-adhesion molecule 1 (MADCAM1), a ligand for LPAM1, is expressed at high levels by the vasculature of mucosal surfaces, allowing for directed migration of GALT-associated lymphocytes to these areas (13,14). Furthermore, C-C motif chemokine ligand 25 (CCL25) expressed by epithelial cells of the small intestine interacts with

C-C motif chemokine receptor 9 (CCR9) on gut derived T-cells, facilitating homing of these lymphocytes to the small bowel (16-18).

The specialized immune cells of the GI tract are present under physiological conditions that contribute to a state of “controlled inflammation.” These immune cells are negatively regulated not to overreact unnecessarily to the intestinal luminal milieu. Mechanisms for the induction of tolerance can be classified as either antigenic ignorance or active tolerance. The former involves preventing microbes and antigen from accessing the immunoreactive areas of the GI tract, while the latter allows induction of both specific and non-specific antigen anti-inflammatory responses and/or deletion of reactive immune cells (19).

The B-cell secretory immunoglobulin (IG) A (sIGA) system and cytokine producing T-cells are principal players for inducing oral tolerance to intestinal bacteria and food antigens. sIGA is the major immunoglobulin isotype found at most mucosal surfaces and is crucial as an anti-inflammatory component due to its ability to bind innocuous antigens and inability to activate complement. These antibodies prevent mucosal penetration of soluble antigen and prohibit microbial colonization, which promotes systemic ignorance of commensal microbes. Deficiencies in the sIGA system have been associated with increased risk of gastrointestinal infection and inflammatory bowel disease (IBD) (20,21). Production of IL4 and IL5 via the type 2 T-helper cell (Th2) response works to enhance sIGA production to stimulate tolerance in the gut (22). These cytokines also act to inhibit the type 1 T-helper cell response (Th1). Increased levels of IL10 and transforming growth factor beta (TGF β) produced by T-cells, along with a suppressed Th1 response, help to generate a tolerogenic environment for commensal microbes in the GI tract.

The decision to induce tolerance or inflammation is directed by professional antigen-presenting cells (APCs). DCs are found in both inductive and effector sites and constitute the main APC in the gut as they are able to efficiently process antigen for activation of naïve T-cells. These mucosal DCs induce regulatory T-cell (Treg) differentiation, act as inducers of effector T-cell response, and assist in maintenance of secondary T-cell responses within inflamed mucosa (23). DC activation occurs once there is exposure to microbial antigens or inflammatory signals. Pattern recognition receptors (PRRs) located on DCs themselves interact with pathogen-associated molecular patterns (PAMPs) expressed by microbes stimulating DCs to mature and migrate to the T-cell areas of lymphoid tissues (24). DCs also recognize and mature in response to inflammatory cytokines such as tumor necrosis alpha (TNF α), IL1, and type 1 interferons (IFNs) (25). Additionally, production of TGF β and IL10 by DCs and T-cells activates B-cells to undergo immunoglobulin class switching from IGM to IGA within PPs which helps to induce an anti-inflammatory response (19).

Tolerogenic or inflammatory responses are only mounted once antigen has come into contact with the GI immune system. Antigen uptake and presentation may occur through several possible routes. As mentioned previously, M-cells in the FAE of PPs can transfer antigen to DCs located in the underlying SED. DCs within the LP express tight junction proteins, allowing for extension of dendrites between epithelial cells for direct antigenic sampling of the intestinal lumen (26). Intestinal epithelial cells (IECs) have been shown to express both major histocompatibility complex (MHC) class II molecules and the nonclassical antigen-presenting molecule cluster of differentiation 1 (CD1), permitting them to present antigen to immune cells that are located in the underlying mucosa (27,28).

The mucosal immune system must efficiently protect the epithelial barrier from invasion by microbes while avoiding a response to antigenic stimuli from commensal bacteria or food proteins that are in constant contact with its surface. Because the majority of antigens that come into contact with these mucosal surfaces are innocuous, the majority of immune responses that are elicited work to simultaneously induce tolerance and subdue inflammation. However, when the control mechanism governing the mucosal immune response go awry, luminal bacteria drive the chronic intestinal inflammation that characterizes IBD.

Role of the Epithelial Barrier in Inflammatory Bowel Disease

IBD represent a heterogeneous group of diseases with two distinct disorders of poorly understood etiology: Crohn's disease (CD) and ulcerative colitis (UC) which are both characterized by chronic intestinal inflammation. Genetic susceptibility, environmental triggers and immune dysregulation have been described as the main factors involved in the establishment and development of IBD. The general hypothesis is that these diseases represent an aberrant immune reaction by the mucosal immune system in response to either pathogenic or resident luminal bacteria (29). According to this hypothesis, resident bacteria can persistently stimulate the mucosal and systemic immune system, thereby perpetuating the inflammatory response. The importance of luminal bacteria in the pathogenesis of IBD draws particular attention to the role played by the intestinal epithelial barrier during the establishment and progression of CD and UC. Compromised integrity of epithelial barrier function has been observed and documented in patients suffering from IBD (30-37).

The surface of the intestinal mucosa consists of a single epithelial cell layer. This epithelial lining functions to protect the underlying tissue compartments from antigens and bacterial products in the lumen. Mucin secreting goblet cells (GCs) create a semi-permeable

mucus-gel layer between the lumen and epithelium. Paneth cells, located adjacent to intestinal stem cells at the crypt base of the small intestine, secrete antimicrobial molecules such as α -defensins, cathelicidins, lysozymes, lipopolysaccharide (LPS)-binding protein, histatins, and lectins into the mucus layer (38-40). Additionally, sIGA antibodies produced by B-cells in the LP are secreted into the mucus by epithelial cells. These antibodies influence the commensal microbiota and contribute substantially to the capacity of the mucus to retain and clear potential pathogens (41). The constituents of the mucus barrier vary throughout the gastrointestinal tract, are rapidly turned over, and can respond dynamically to potentially infectious organisms. Aberrant changes in mucin production or structure influence their protective functions and therefore constitute possible etiological factors in the pathogenesis of IBD. Indeed, it has been shown that some patients with IBD have alterations in both membrane-bound and secretory mucins (42,43).

The intestinal barrier must be selectively permeable to allow for entry of luminal nutrients, ions, and water while restricting pathogen access to underlying tissues. Beyond the mucus layer, the barrier function of IECs is regulated by a network of intracellular junctional protein complexes. The apical-most tight junctions (TJs) consist of proteins that physically seal but also form channels to allow for permeation of molecules between cells. These TJ proteins include occludin (OCLN), claudins (CLDNs), junctional adhesion molecules (JAMs), and zonula occludens (ZOs) (Fig. 1.1). TJs are regulated in their molecular composition and function by intracellular scaffolding proteins and the cytoskeleton (44). Visualization of TJs reveals a series of anastomosing intramembranous strands in which strand complexity correlates with tightness of the epithelial barrier (45). Investigations using freeze-fracture microscopy report an increased distance between enterocytes, and a decrease in the number and complexity of TJ strands in CD

and UC patients (46-48). Additionally, immunohistochemistry and protein analysis have demonstrated a substantial loss of OCLN from the TJs in the colonic mucosa of patients with CD and UC (49).

Evidence from experimentally induced colitis models has also established the role of TJs in the pathogenesis of IBD. Colitis induction using dextran sodium sulfate (DSS) has demonstrated that mice with non-functional mutations in the *Clcn2* gene have amplified disease severity that manifests with increased disease activity indices, increased loss of body weight, extensive histopathological changes, decreased baseline transepithelial electrical resistance (TER), and increased permeability to mannitol in the small intestine (50). *Clcn2* encodes the voltage-gated CLC2 chloride channel and belongs to the CLC super family, which consists of several isoforms of voltage-gated Cl⁻ channels that are expressed in a wide variety of tissues and organs (51). CLC2 helps to modulate barrier function and is located predominately at the apical TJs of the small intestine where it is necessary for repair of the paracellular barrier in the event of injury to the epithelium (52-55).

Situated below the apical TJ is the adherens junction (AJ) (Fig. 1.1). This junctional complex is responsible for initiating and maintaining cell-cell contact and for cell-cell recognition (56). AJs are organized with a series of transmembrane proteins (cadherins, CDHs) that are associated with the underlying actin cytoskeleton via cytoplasmic plaque proteins (catenin family, CTNNs) (56,57). Reduced expression of the transmembrane protein E-cadherin (CDH1) and plaque protein α -catenin (CTNNA1), as well as dysregulation of CDH1 and P-cadherin (CDH3), has been documented in the inflamed epithelium of both CD and UC patients (58-60).

Cytokines are key regulators of the dynamic nature of the intracellular junctional complexes. The pro-inflammatory cytokines TNF α and interferon gamma (IFN γ) have been shown to decrease epithelial barrier function across model epithelial cell lines such as T84, Caco-2, and HT29 cells (61-65). Redistribution of the TJ transmembrane proteins OCLN, CLDN1, CLDN4, and JAMA has been documented in T84 cells in response to IFN γ with effects significantly potentiated in the presence of TNF α (65-67). On the other hand, the anti-inflammatory cytokines IL10 and TGF β have been shown to serve a protective role in the maintenance of barrier function of the intestinal epithelial cell junctions (23). Findings such as these emphasize the role of inflammatory stimuli on the disassembly and disruption of junctional complexes.

The epithelial barrier protects the intestine from harmful antigens. IECs produce a wide array of molecules that play a role in initiating, maintaining, but also preventing and controlling mucosal inflammation. A defect in epithelial cell-regulated barrier function may lead to continued exposure of intestinal immune cells to bacterially derived molecules leading to the destructive intestinal inflammation that characterizes IBD.

Genetic Contributions to Inflammatory Bowel Disease Pathogenesis

Because IBD is a complex disease that results from variation within multiple genes and their interaction with behavioral and environmental factors, it does not follow readily predictable patterns of inheritance. The availability of genetic maps and the identification of markers scattered throughout the genome have enabled quantitative trait loci (QTL) mapping. The basic principle behind simple QTL mapping is to find polymorphisms that display a statistical difference in the trait mean between individuals of different genotypes. Utilization of QTL mapping allows complex phenotypes to be linked to specific regions of chromosomes. Linkage

and association studies in humans have provided insight into the genetic factors that contribute to the pathogenesis of IBD. The former seeks to identify marker loci that co-segregate with the disease within families, while the latter seeks to identify particular variants observed at higher allelic frequencies in IBD patients compared to case-matched controls in a given population. Both approaches have been utilized to characterize multiple likely disease associations in IBD.

Clustering of IBD cases within families reflects shared genetic, developmental and environmental contributions. Relatives of UC and CD probands have a demonstrated 8-10-fold greater risk of manifesting IBD symptoms (68), and having a first-degree relative with CD or UC confers a greater risk than any known environmental factor (69). Comparing the concordance rates between monozygotic (MZ) and dizygotic (DZ) twins provides a means of defining the significance of genetic factors. Data from published IBD twin studies gives a range of concordance rates for MZ twins at 20-55% for CD and 6.3–17% for UC; DZ twins at 0–3.6% for CD and 0-6.3% for UC (70). MZ concordance rates in comparison to DZ concordance rates are generally higher in CD cases than in UC cases which supports the general concept that genetic factors play a more significant role in CD pathogenesis. The risk to first-degree relatives of a CD proband of developing UC (or conversely) is also increased but significantly lower than that for the same disease (23). These data support that some risk alleles are specific to either IBD condition, whereas others are common to both disorders.

More recently, there have been important advances in the understanding of genetic contributions to IBD due to technological progress in genetic testing and DNA sequencing that has allowed genome-wide association studies (GWAS) to aid in the identification of new single nucleotide polymorphisms (SNPs). The conceptual basis of GWAS is that most complex genetic disorders are polygenic and are driven by various common genetic polymorphisms. Multiple

GWAS performed on a variety of distinct chronic immune-mediated diseases found overlap of general genomic regions associated with each disease, leading to the development of the ImmunoChip (71). This custom-made chip contains a dense map of markers clustered in 186 regions that demonstrate genome-wide significance for association in at least one autoimmune or chronic inflammatory disease (71). A meta-analysis combining GWAS with ImmunoChip data identified 163 loci associated with IBD. Of these loci, 30 conferred risk to CD, 23 conferred risk to UC, and 110 conferred risk to both IBD subtypes. The identified loci explained 13.6% of CD and 7.5% of UC total disease variances, respectively (72) (Table 1.1). With few exceptions, the associated genomic regions identified via GWAS have not yielded specific causative genes or functional alleles for the pathogenesis of IBD. Many of the loci associated with IBD contain multiple genes or no genes at all. Missense polymorphisms conserved between species and predicted to alter protein structure and/or function are strong candidates for functional, disease-associated polymorphisms. However, it is anticipated that many of the most important risk alleles for complex multigenic disorders, such as IBD, will involve noncoding region variation that affects gene regulation and function.

GWAS data can also be used to calculate heritability from the additive genetic variance attributed to all identified SNP (SNP effects). Estimates of heritability of liability for CD and UC, calculated from imputed SNP effects of the GWAS/ImmunoChip meta-analysis, are 0.37 and 0.27, respectively (70,72). The assumption that genetic and environmental factors act independently of one another still underpins the mathematical models used to estimate heritability. The true interaction between genes and the environment involves a multidirectional interplay, mediated by the microbiota, epigenome, and innate and acquired immune system, which further complicates elucidation of IBD etiology.

Linkage studies and GWAS have successfully identified susceptibility loci for IBD. The identification of these loci has enhanced understanding of the underlying causes of the disorder by providing important clues for crucial and disrupted pathways of the intestinal immune system. Reported observations indicate that there is no major gene, with a large effect on the phenotype variance for IBD. Thus, the model of inheritance derived from genome-wide scans is a complex interplay between many genetic risk factors, each with a modest individual contribution. A given IBD susceptibility gene is neither necessary nor sufficient for disease development.

With the current number of loci associated with IBD and the promise of more to come as next generation sequencing studies grow, attention is now turning to the identification of causal genes and variants within these loci (fine-mapping). Historically, follow-up of genetic associations has proceeded via time-consuming experimental validation of proposed genes using cellular or animal models. Murine models have been indispensable in defining mechanisms of disease pathogenesis, suggesting candidate genes for human disease, and designing new therapeutic strategies for the treatment of patients with IBD. Similarities in pathological findings between experimentally-induced IBD and IBD symptoms in humans are well-established (73).

Animal Models of Inflammatory Bowel Disease

The identification of mechanisms involved in intestinal injury is essential for the development of prevention and mitigation strategies. Utilization of data gathered from human studies of intestinal disease would provide the most reliable data; however, there are particular difficulties associated with research involving human subjects. There are often complex ethical considerations surrounding the collection and use of human tissue. Furthermore, the pronounced genetic variability between individuals limits the generalizability of results collected from particular human studies to the population as a whole. As such, comparative animal models are

used to provide representative information underlying the pathogenesis of intestinal disease in people. Several different animal models of IBD exist, as no single model captures the complexity of human IBD. Mice are the most commonly used animal model for intestinal studies (74) due to the many similarities between mice and humans, including gene homology, intestinal structure and function, immune response, and intestinal bacterial community composition (75). Additional advantages to using mice as an animal model include their small size, relatively short estrous cycles and gestation period, large litter sizes, abundance of analysis techniques, genetically homogeneous backgrounds, and increasing availability of genetic tools.

Mouse models can be categorized as chemically-induced, spontaneous colitis, genetically engineered, and transgenic models, with each providing valuable insights into one or another major aspect of disease (Figure 1.2). Experimentally induced inflammation allows for control over both genetic and environmental factors that may influence pathological findings associated with IBD, such as a dysregulated response of the innate and adaptive immune systems, loss of tolerance to commensal bacteria, disrupted mucosal barrier function, increased inflammatory mediators, and oxidative stress.

The intestinal mucosa normally functions to maintain a balance of pro-inflammatory cells, with pathways of cytokine synthesis and cytokine-induced signal transduction being tightly regulated by complex feedback mechanisms and Tregs (76,77). In IBD, immunologic response to commensal bacterial antigens is dysregulated, which results in a dramatic shift/imbalance in the cytokine production profile thought to be represented by Th1 and Th2 patterns of expression (78). In humans, UC is typically characterized by a Th2 driven immune response as indicated by marked increases in IL4, IL5, IL10, and IL23 (79-83) with significant thickening and dense infiltration of immune effector cells into the mucosa and LP of the bowel wall (84). Conversely,

CD patients present with increased production of IL12, IFN γ , TNF α , and IL2 which is indicative of a predominately Th1 immune response. Thickening and transmural infiltration of immune cells extends beyond the mucosa into the submucosa of those affected by CD (84). Recent studies showing upregulation of TNF α (Th1 profile) in UC and IL5 (Th2 profile) in CD have challenged the polarization concept of a strict Th1/Th2 pattern (85-87). Of additional importance is the increasing interest in the role of the Th17 pathway (IL23 and IL17) in the manifestation of intestinal inflammation (78,88). Experimental models of inflammation, however, are usually subject to the Th1/Th2 paradigm in that they typically resolve into a Th1 or Th2 pathway of responsiveness similar to that seen in the human IBD conditions (89).

Chemical-induced colitis models (dextran sodium sulfate (DSS), 2,4,6-trinitrobenzene sulfonic acid (TNBS), oxazolone, nonsteroidal anti-inflammatory drugs (NSAIDs), carrageenan, and peptidoglycan-polysaccharide (PGPS) are among the most extensively used as they offer reproducibility, along with ease of development and use. DSS-induced colitis, the most widely used of the chemical models, morphologically and symptomatically resembles UC in humans (90,91). It has been demonstrated that acute inflammation in DSS converts to a predominantly Th-2 mediated response in the chronic state with noted decreases in levels of TNF α , IL17 and elevated levels of IL4, IL6, IL10 and IFN γ (78,92). Alternatively, TNBS-induced colitis is a popular choice for recapitulation of CD as administration of monoclonal anti-IL12 antibody not only prevents development of colitis, but also is a highly effective treatment after colitis is established (93), confirming that TNBS colitis is a Th1 mediated response driven by IL12-induced inflammation. Furthermore, a trial of anti-IL12 as a therapeutic agent in humans with CD provided initial evidence that anti-IL12 administration is an effective treatment for this disease (94), likely via induction of apoptosis of effector T-cells mediated in part by Fas/Fas

ligand interactions (95). Additionally, the prominent role of TNF α in CD is also found in the TNBS model, as colitis could not be induced in *Tnf α* knockout (KO) mice and increased in severity in mice over-expressing TNF α as the result of the introduction of a *Tnf α* transgene (96).

DSS, a synthetic sulfated polysaccharide composed of dextran and a sulfated anhydro-glucose unit, is directly toxic to colonic epithelium (73). Contact with DSS causes epithelial cell injury and destabilizes protective mucus layers, resulting in altered mucosal barrier function throughout the colonic epithelium (97,98). Disruption of the intestinal epithelial monolayer leads to entry of luminal bacteria and associated antigens into the mucosa, which allows introduction of proinflammatory intestinal contents into underlying tissue (92,99-104). For induction of murine colitis, 40-50 kDa DSS is provided in the drinking water and commonly administered at a dosage of 3–10% for 7–10 days to induce acute inflammation (101,105-107). Prolonged exposure may be used to progress acute colitis to chronic colitis by administering in 3-5 cycles with a rest period of 1-2 weeks between cycles. Animals in the acute phase present with weight loss, diarrhea, occult blood in stools, and anemia (73). These clinical symptoms are accompanied by histological changes such as mucin depletion, epithelial degeneration, ulcerations, infiltration of granulocytes, goblet cell depletion, and necrosis leading to disappearance of epithelial cells, which results in the formation of cryptitis and crypt abscesses (73,108).

TNBS, a haptenizing agent, initiates mucosal immune responses by rendering colonic proteins immunogenic to the host immune system (109). Experimentally, a dosage of 50-150 mg/kg TNBS is dissolved in ethanol and delivered intrarectally via catheter to induce colitis (110). Ethanol serves as a carrier for TNBS and helps to induce inflammation by breaking the mucosal barrier (93,111). TNBS treated animals present with many of the same symptoms as the DSS model: inconsistent stool formation, occult, and bloody diarrhea (110). Mucosal edema,

distortion of crypts and the formation of abscesses also occur during the course of the disease (112,113). At a microscopic level, inflammation spreads transversely, leading to the development of transmural colitis, which is a shared feature and hallmark of human CD (110,114).

A major insight into IBD pathophysiology in humans is that host genetic background determines susceptibility to the development of colitis (115). Differences in susceptibility to both DSS and TNBS-induced colitis due to genetic background are also well established (110,116-118). For example, C3HeJ, C3H/HeJBir, and C57BL/6 mice are highly susceptible to DSS-induced colitis, while BALB/c mice are more resistant and only develop colitis when higher percentages of DSS are administered (116,119). Additionally, C57BL/6 mice develop a severe chronic inflammation after administration of DSS for 5 days, whereas BALB/c mice resolve symptoms of colitis after the acute phase (119). Similarly, when treated with TNBS, mice from SJL/J, C3HeJ and BALB/c backgrounds develop CD-like intestinal lesions, while C57BL/6 mice under the same conditions remain relatively unaffected (120). Furthermore, the ability to mount an IL12 response to LPS exposure has been identified as a determining factor in susceptibility to TNBS-induced colitis between SJL/J (susceptible) and C57BL/6 (resistant) mice, as IL12 is a major cytokine involved in the differentiation of Th1-CD4+ T cells (118,121). Because certain strains of mice are more suited to investigate specific conditions of IBD pathogenesis, it is imperative to choose strains that best represent aspects of the disease being examined. However, this is a consideration often overlooked by researchers when choosing an appropriate animal model to recapitulate human disease. Identification of differences in the response to experimentally induced inflammation among inbred strains of mice could provide the basis for identification and validation of the genes determining susceptibility or resistance to colitis.

Relevance of this Research Project

The opposite responses of BALB/c and C57BL/6 mice to DSS and TNBS-induced colitis were of particular interest for this research project. As mentioned previously, C57BL/6 mice are highly susceptible to DSS-induced colitis, while BALB/c mice demonstrate a marked resistance to developing inflammation under this model. In comparison, BALB/c mice are highly susceptible to TNBS-induced colitis, while C57BL/6 mice develop minimal signs of colitis when TNBS is administered intrarectally.

In chapter 2, we investigated the effect of genetic background on intestinal permeability in both models and found that barrier function in susceptible C57BL/6 mice is significantly and persistently impaired in the DSS-induced colitis model. However, the same does not hold true for susceptible BALB/c mice when colitis is induced via exposure to TNBS. No significant changes in intestinal barrier function were detected in BALB/c animals despite the presence of physiological markers of inflammation (decreased body weight, bloody stool, and diarrhea) in this model. First filial generation (F1) hybrid mice (CB6F1/J), which were the offspring of a cross between BALB/c females and C57BL/6 males were also exposed to both DSS and TNBS. We observed intermediate phenotypes for weight loss and/or disease severity scores for our CB6F1/J mice in the two chemically-induced models of colitis. Intestinal permeability remained unaltered in these F1 mice under both experimental conditions.

In chapter 3, we utilized our CB6F1/J mice to generate a F2 QTL mapping population (F2CB). Severity of inflammation was assessed via measurements of disease activity scores (stool consistency and fecal blood), as well as body weight loss scores. Percent body weight was strongly correlated to overall disease activity and was used as the phenotype of interest for the QTL analysis. We were unable to identify significant QTL in either model, but several

suggestive QTL were identified that were exclusive to each model. We discuss potential approaches to increase the power to detect significant QTL in our experimental design. The use of a combinatorial methodology based on transcriptome and mapping data to reduce the number of candidate genes in potentially identified QTL regions is also proposed.

In chapter 4, we discuss the how the implementation of 16S ribosomal phylogenetic analysis of fecal samples collected from parental strains and F2CB mice may be helpful in determining the effect of genetic background on the composition of the gut microbiota and for identifying microbial species that may be relevant to human IBD. Follow-up studies are also suggested to address potential limitations of the research previously conducted and to gather new data that may be informative for the overall characterization of both the DSS and TNBS models.

Identifying the most appropriate animal model to study intestinal inflammation is an important consideration. It requires researchers to proactively consider the advantages and disadvantages of each model in order to determine the most suitable model(s) for addressing the specific aspects of the inflammatory response being investigated. Ultimately, the projects discussed here will help to elucidate the fundamental processes involved in the onset and progression of acute and chronic inflammation in two of the most popular models of IBD. These findings will aid in illuminating the limitations, benefits, differences, and similarities between various animal models, which are an essential component for developing a complete understanding of the complex etiology of IBD. Effectively applied animal models are instrumental for the identification of novel risk loci, validation of potential genes of interest, and development of appropriate mitigation strategies/treatment options for human patients.

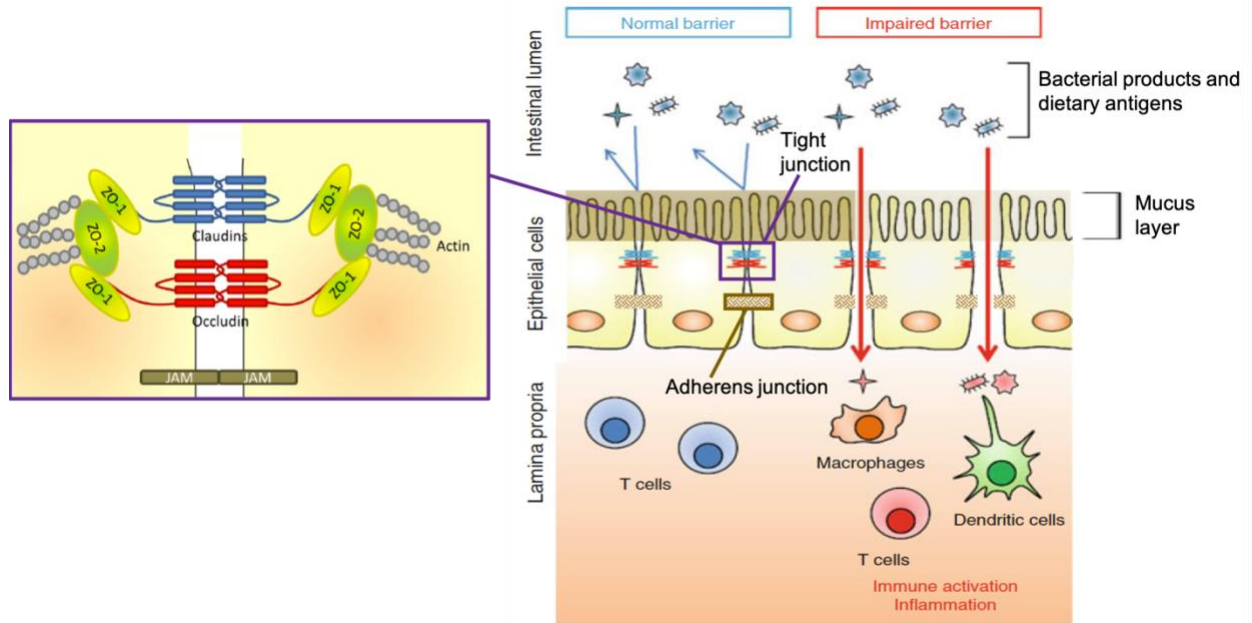


Figure 1.1: Intestinal barrier function. The epithelium provides a physical barrier to luminal bacteria, toxins, and antigens. The barrier is organized by different components, including the tight and adherens junctions which regulate the paracellular passages of ions, solutes, and water between adjacent cells. Barrier impairment allows the passage of noxious molecules, which can induce the excessive activation of mucosal immune cells and inflammation. Figure adapted from (122,123).

Mouse Models

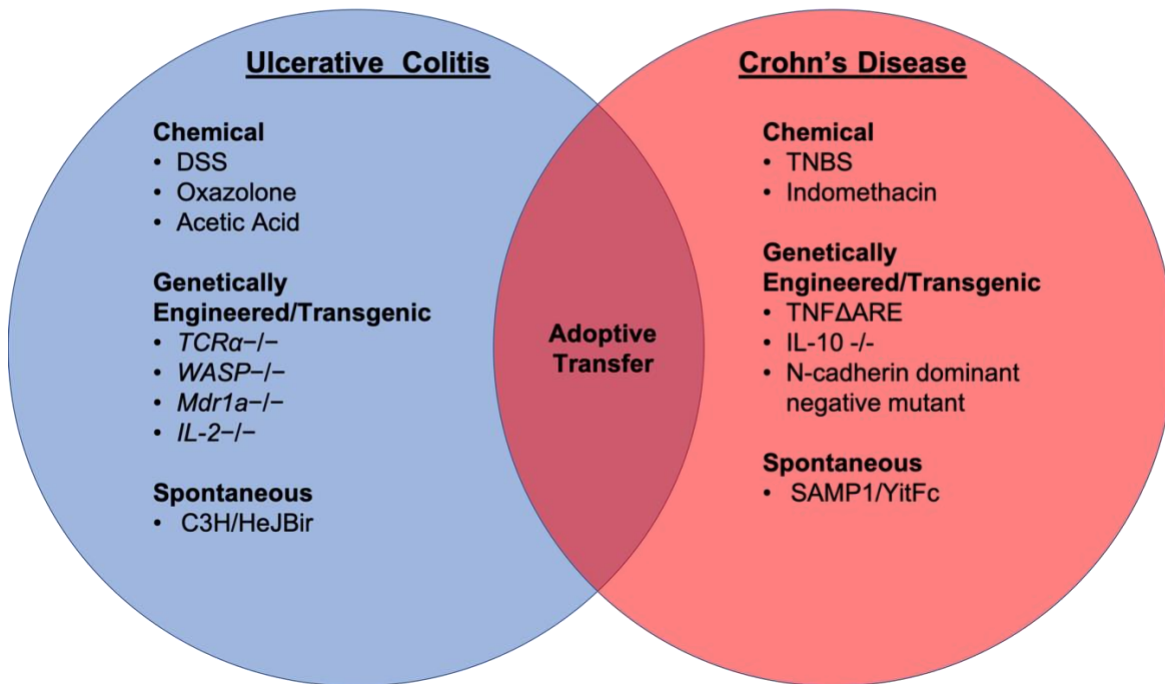


Figure 1.2: Mouse models of IBD. Representative models that mimic the characteristics of the two major subtypes of IBD (Ulcerative Colitis [UC] and Crohn's disease [CD]) are shown. Figure adapted from (124).

Table 1.1 Summary of significant CD, UC, and general IBD loci identified by GWAS. The position given in megabases (Mb) is the middle of the locus region, with all positions relative to human reference genome GRCh37. Listed genes have been implicated by one or more candidate gene approaches. Table adapted from (72).

Chromosome	Position (Mb)	SNP	Type	Candidate Genes [number of additional genes in locus]
1	1.24	rs12103	IBD	<i>TNFRSF18, TNFRSF4</i> , [30]
1	2.5	rs10797432	UC	<i>TNFRSF14, MMEL1, PLCH2</i> , [8]
1	8.02	rs35675666	IBD	<i>TNFRSF9</i> , [6]
1	20.15	rs6426833	UC	[9]
1	22.7	rs12568930	IBD	[3]
1	67.68	rs11209026	IBD	<i>IL23R, IL12RB2</i> , [4]
1	70.99	rs2651244	IBD	[3]
1	78.62	rs17391694	CD	[5]
1	114.3	rs6679677	CD	<i>PTPN22, DCLRE1B</i> , [7]
1	120.45	rs3897478	CD	<i>ADAM30</i> , [5]
1	151.79	rs4845604	IBD	<i>RORC</i> , [14]
1	155.67	rs670523	IBD	<i>UBQLN4, RIT1, MSTO1</i> , [28]
1	160.85	rs4656958	IBD	<i>CD48, SLAMF1, ITLN1, CD244, F11R, USF1, SLAMF7, ARHGAP30</i> , [8]
1	161.47	rs1801274	IBD	<i>FCGR2A, FCGR2B, FCGR3A, HSPA6, FCGR3B, FCRLA</i> , [9]
1	172.85	rs9286879	CD	<i>FASLG, TNFSF18</i> , [0]
1	197.6	rs2488389	IBD	<i>C1orf53</i> , [2]
1	200.09	rs2816958	UC	[3]
1	200.87	rs7554511	IBD	<i>KIF21B</i> , [6]
1	206.93	rs3024505	IBD	<i>IL10, IL20, IL19, IL24, PIGR, MAPKAPK2, FAIM3, RASSF5</i> , [3]
2	25.12	rs6545800	IBD	<i>ADCY3</i> , [6]
2	27.63	rs1728918	CD	<i>UCN</i> , [23]
2	28.61	rs925255	IBD	<i>FOSL2, BRE</i> , [1]
2	43.81	rs10495903	IBD	[5]
2	61.2	rs7608910	IBD	<i>REL, C2orf74, KIAA1841, AHSA2</i> , [6]
2	62.55	rs10865331	CD	[3]
2	65.67	rs6740462	IBD	<i>SPRED2</i> , [1]
2	102.86	rs917997	IBD	<i>IL1R2, IL18RAP, IL18R1, IL1R1, IL1RL1, IL1RL2</i> , [3]
2	163.1	rs2111485	IBD	<i>IFIH1</i> , [5]
2	191.92	rs1517352	IBD	<i>STAT1, STAT4</i> , [2]

Table 1 (continued)

2	198.65	rs1016883	UC	<i>RFTN2, PLCL1, [7]</i>
2	199.7	rs17229285	UC	<i>[0]</i>
2	219.14	rs2382817	IBD	<i>SLC11A1, CXCR2, CXCR1, PNKD, ARPC2, TMBIM1, CTDSP1, [8]</i>
2	231.09	rs6716753	CD	<i>SP140, [5]</i>
2	234.145	rs12994997	CD	<i>ATG16L1, INPP5D, [7]</i>
2	241.57	rs3749171	IBD	<i>GPR35, [12]</i>
3	18.76	rs4256159	IBD	<i>[0]</i>
3	48.96	rs3197999	IBD	<i>MST1, PFKFB4, MST1R, UCN2, GPX1, IP6K2, BSN, IP6K1, USP4, [56]</i>
3	53.05	rs9847710	UC	<i>PRKCD, ITIH4, [8]</i>
4	48.36	rs6837335	CD	<i>TXK, TEC, SLC10A4, [3]</i>
4	74.85	rs2472649	IBD	<i>CXCL5, CXCL1, CXCL3, IL8, CXCL6, PF4, CXCL2, PF4V1, [3]</i>
4	102.86	rs13126505	CD	<i>[1]</i>
4	103.51	rs3774959	UC	<i>NFKB1, MANBA, [2]</i>
4	123.22	rs7657746	IBD	<i>IL2, IL21, [2]</i>
5	0.59	rs11739663	UC	<i>SLC9A3, [8]</i>
5	10.69	rs2930047	IBD	<i>DAP, [2]</i>
5	40.38	rs11742570	IBD	<i>PTGER4, [1]</i>
5	55.43	rs10065637	CD	<i>IL6ST, IL31RA, [1]</i>
5	72.54	rs7702331	CD	<i>[4]</i>
5	96.24	rs1363907	IBD	<i>ERAP2, ERAP1, LNPEP, [2]</i>
5	130.005	rs4836519	IBD	<i>[1]</i>
5	131.19	rs2188962	IBD	<i>IRF1, IL13, CSF2, SLC22A4, IL4, IL3, IL5, PDLIM4, SLC22A5, ACSL6, [8]</i>
5	134.44	rs254560	UC	<i>[6]</i>
5	141.51	rs6863411	IBD	<i>SPRY4, NDFIP1, [5]</i>
5	150.27	rs11741861	IBD	<i>TNIP1, IRGM, ZNF300P1, [8]</i>
5	158.8	rs6871626	IBD	<i>IL12B, [3]</i>
5	173.34	rs17695092	CD	<i>CPEB4, [2]</i>
5	176.79	rs12654812	IBD	<i>DOK3, [17]</i>
6	14.71	rs17119	IBD	<i>[0]</i>
6	20.77	rs9358372	IBD	<i>[2]</i>
6	21.42	rs12663356	CD	<i>[3]</i>
6	31.27	rs9264942	CD	<i>HLA [C, PSORS1C1, NFKBIL1, MICB, [18]</i>
6	32.595	rs6927022	UC	<i>HLA [DQB1, HLA [DRB1, HLA [DQA1, HLA [DRA, [12]</i>

Table 1 (continued)

6	90.96	rs1847472	IBD	[1]
6	106.43	rs6568421	IBD	[2]
6	111.82	rs3851228	IBD	<i>TRAF3IP2, FYN, REV3L</i> , [2]
6	127.45	rs9491697	CD	[3]
6	128.24	rs13204742	CD	[2]
6	138	rs6920220	IBD	<i>TNFAIP3</i> , [1]
6	143.9	rs12199775	IBD	<i>PHACTR2</i> , [5]
6	159.49	rs212388	CD	<i>TAGAP</i> , [5]
6	167.37	rs1819333	IBD	<i>CCR6, RPS6KA2, RNASET2</i> , [3]
7	2.78	rs798502	UC	<i>CARD11, GNA12, TTYH3</i> , [4]
7	27.22	rs4722672	UC	[14]
7	28.17	rs864745	CD	<i>CREB5, JAZF1</i> , [1]
7	50.245	rs1456896	IBD	<i>ZBPB, IKZF1</i> , [4]
7	98.75	rs9297145	IBD	<i>SMURF1</i> , [6]
7	100.335	rs1734907	IBD	<i>EPO</i> , [21]
7	107.45	rs4380874	UC	<i>DLD</i> , [9]
7	116.89	rs38904	IBD	[6]
7	128.57	rs4728142	UC	<i>IRF5, TNPO3, TSPAN33</i> , [11]
7	26.88	rs10486483	CD	[2]
8	90.87	rs7015630	CD	<i>RIPK2</i> , [4]
8	126.53	rs921720	IBD	<i>TRIB1</i> , [1]
8	129.56	rs6651252	CD	[0]
8	130.62	rs1991866	IBD	[2]
9	4.98	rs10758669	IBD	<i>JAK2</i> , [4]
9	93.92	rs4743820	IBD	<i>NFIL3</i> , [2]
9	117.6	rs4246905	IBD	<i>TNFSF8, TNFSF15, TNC</i> , [2]
9	139.32	rs10781499	IBD	<i>CARD9, PMPCA, SDCCAG3, INPP5E</i> , [19]
10	6.08	rs12722515	IBD	<i>IL2RA, IL15RA</i> , [6]
10	30.72	rs1042058?	IBD	<i>MAP3K8</i> , [3]
10	35.295	rs11010067	IBD	<i>CREM</i> , [3]
10	59.99	rs2790216	IBD	<i>CISD1, IPMK</i> , [2]
10	64.51	rs10761659	IBD	[3]
10	75.67	rs2227564	IBD	[13]
10	81.03	rs1250546	IBD	[5]
10	82.25	rs6586030	IBD	<i>TSPAN14, C10orf58</i> , [4]
10	94.43	rs7911264	IBD	[4]
10	101.28	rs4409764	IBD	<i>NKX2-3</i> , [6]
11	1.87	rs907611	IBD	<i>TNNI2, LSPI</i> , [17]

Table 1 (continued)

11	58.33	rs10896794	IBD	<i>CNTF, LPXN, [8]</i>
11	60.77	rs11230563	IBD	<i>CD6, CD5, PTGDR2, [12]</i>
11	61.56	rs4246215	IBD	<i>C11orf9, FADS1, FADS2, [12]</i>
11	64.12	rs559928	IBD	<i>CCDC88B, RPS6KA4, TRPT1, FLRT1, [20]</i>
11	65.65	rs2231884	IBD	<i>RELA, FOSL1, CTSW, SNX32, [22]</i>
11	76.29	rs2155219	IBD	<i>[5]</i>
11	96.02	rs483905	UC	<i>JRKL, MAML2, [2]</i>
11	114.38	rs561722	UC	<i>FAM55A, FAM55D, [5]</i>
11	118.74	rs630923	IBD	<i>CXCR5, [17]</i>
12	12.65	rs11612508	IBD	<i>LOH12CRI, [8]</i>
12	40.77	rs11564258	IBD	<i>LRRK2, MUC19</i>
12	48.2	rs11168249	IBD	<i>VDR, [8]</i>
12	68.49	rs7134599	IBD	<i>IFNG, IL26, IL22, [1]</i>
13	27.52	rs17085007	IBD	<i>[2]</i>
13	40.86	rs941823	IBD	<i>[3]</i>
13	44.45	rs3764147	CD	<i>LACCI, [3]</i>
13	99.95	rs9557195	IBD	<i>GPR183, GPR18, [6]</i>
14	69.27	rs194749	IBD	<i>ZFP36L1, [4]</i>
14	75.7	rs4899554	IBD	<i>FOS, MLH3, [6]</i>
14	88.47	rs8005161	IBD	<i>GPR65, GALC, [1]</i>
15	38.89	rs16967103	CD	<i>RASGRP1, SPRED1, [2]</i>
15	41.55	rs28374715	UC	<i>ITPKA, NDUFAF1, NUSAP1, [8]</i>
15	67.43	rs17293632	IBD	<i>SMAD3, [2]</i>
15	91.17	rs7495132	IBD	<i>CRTC3, [3]</i>
16	11.54	rs529866	IBD	<i>SOCS1, LITAF, RMI2, [10]</i>
16	23.86	rs7404095	IBD	<i>PRKCB, [5]</i>
16	28.595	rs26528	IBD	<i>RABEP2, IL27, EIF3C, SULT1A1, SULT1A2, NUPR1, [9]</i>
16	30.47	rs11150589	UC	<i>ITGAL, [20]</i>
16	50.66	rs2066847	CD	<i>NOD2, ADCY7, [5]</i>
16	68.58	rs1728785	UC	<i>ZFP90, [6]</i>
16	86	rs10521318	IBD	<i>IRF8, [4]</i>
17	25.84	rs2945412	CD	<i>LGALS9, NOS2, [3]</i>
17	32.59	rs3091316	IBD	<i>CCL13, CCL2, CCL11, [4]</i>
17	37.91	rs12946510	IBD	<i>IKZF3, ZBP2, GSDMB, ORMDL3, GSDMA, [12]</i>
17	40.53	rs12942547	IBD	<i>STAT3, STAT5B, STAT5A, [13]</i>
17	57.96	rs1292053	IBD	<i>TUBD1, RPS6KB1, [9]</i>

Table 1 (continued)

17	70.64	rs7210086	UC	[3]
18	12.8	rs1893217	IBD	[6]
18	46.39	rs7240004	IBD	<i>SMAD7</i> , [2]
18	67.53	rs727088	IBD	<i>CD226</i> , [2]
19	1.12	rs2024092	CD	<i>GPX4</i> , <i>HMHA1</i> , [20]
19	10.49	rs11879191	IBD	<i>TYK2</i> , <i>PPAN</i> [<i>P2RY11</i> , <i>ICAM1</i> , [25]
19	33.73	rs17694108	IBD	<i>CEBPG</i> , [8]
19	46.85	rs4802307	CD	[9]
19	47.12	rs1126510	UC	<i>CALM3</i> , [14]
19	49.2	rs516246	CD	<i>DBP</i> , <i>SPHK2</i> , <i>IZUMO1</i> , <i>FUT2</i> , [22]
19	55.38	rs11672983	IBD	<i>NLRP7</i> , <i>NLRP2</i> , <i>KIR2DL1</i> , <i>LILRB4</i> , [15]
20	30.75	rs6142618	IBD	<i>HCK</i> , [10]
20	31.37	rs4911259	IBD	<i>DNMT3B</i> , [8]
20	33.8	rs6088765	UC	<i>PROCR</i> , <i>UQCC</i> , <i>CEP250</i> , [8]
20	43.06	rs6017342	UC	<i>ADA</i> , <i>HNF4A</i> , [9]
20	44.74	rs1569723	IBD	<i>CD40</i> , <i>MMP9</i> , <i>PLTP</i> , [11]
20	48.95	rs913678	IBD	<i>CEBPB</i> , [5]
20	57.82	rs259964	IBD	<i>ZNF831</i> , <i>CTSZ</i> , [5]
20	62.34	rs6062504	IBD	<i>TNFRSF6B</i> , <i>LIME1</i> , <i>SLC2A4RG</i> , <i>ZGPAT</i> , [23]
21	16.81	rs2823286	IBD	[0]
21	34.77	rs2284553	CD	<i>IFNGR2</i> , <i>IFNAR1</i> , <i>IFNAR2</i> , <i>IL10RB</i> , <i>GART</i> , <i>TMEM50B</i> , [6]
21	40.46	rs2836878	IBD	[3]
21	45.62	rs7282490	IBD	<i>ICOSLG</i> , [9]
22	21.92	rs2266959	IBD	<i>MAPK1</i> , <i>YDJC</i> , <i>UBE2L3</i> , <i>RIMBP3</i> , <i>CCDC116</i> , [8]
22	30.425	rs2412970	IBD	<i>LIF</i> , <i>OSM</i> , <i>MTMR3</i> , [8]
22	39.69	rs2413583	IBD	<i>ATF4</i> , <i>TAB1</i> , <i>APOBEC3G</i> , [16]

References

- (1) Sanchez MI, Bercik P. Epidemiology and Burden of Chronic Constipation. *Canadian journal of gastroenterology* 2011;25 Suppl B (suppl b):15B.
- (2) Hunt R, Quigley E, Abbas Z, Eliakim A, Emmanuel A, Goh K, et al. Coping with Common Gastrointestinal Symptoms in the Community: A Global Perspective on Heartburn, Constipation, Bloating, and Abdominal Pain/Discomfort May 2013. *Journal of Clinical Gastroenterology* 2014 Aug;48(7):567-578.
- (3) Ahmed SM, Hall AJ, Robinson AE, Verhoef L, Premkumar P, Parashar UD, Koopmans M, Lopman BA. Global prevalence of norovirus in cases of gastroenteritis: a systematic review and meta-analysis. *Lancet Infectious Diseases*, The 2014;14(8):725-730.
- (4) Liu L, Johnson HL, Cousens S, Perin J, Scott S, Lawn JE, Rudan I, Campbell H, Cibulskis R, Li M, Mathers C, Black RE. Global, regional, and national causes of child mortality: an updated systematic analysis for 2010 with time trends since 2000. *Lancet*, The 2012;379(9832):2151-2161.
- (5) Molodecky NA, Soon IS, Rabi DM, Ghali WA, Ferris M, Chernoff G, Benchimol EI, Panaccione R, Ghosh S, Barkema HW, Kaplan GG. Increasing Incidence and Prevalence of the Inflammatory Bowel Diseases with Time, Based on Systematic Review. *Gastroenterology* 2012;142(1): 54.e42.
- (6) Ponder A, Long MD. A clinical review of recent findings in the epidemiology of inflammatory bowel disease. *Clinical epidemiology* 2013; 5:237-247.
- (7) Mowat AM. Anatomical basis of tolerance and immunity to intestinal antigens. *Nature Reviews.Immunology* 2003;3(4):331-41.
- (8) Masopust D, Vezys V, Marzo AL, Lefrancois L. Preferential Localization of Effector Memory Cells in Nonlymphoid Tissue. *Science* 2001 Mar 23;291(5512):2413-2417.
- (9) Kraehenbuhl J, Neutra MR. EPITHELIAL M CELLS: Differentiation and Function. *Annual Review of Cell and Developmental Biology* 2000 Nov;16(1):301-332.
- (10) Suzuki K, Oida T, Hamada H, Hitotsumatsu O, Watanabe M, Hibi T, et al. Gut Cryptopatches: Direct Evidence of Extrathymic Anatomical Sites for Intestinal T Lymphopoiesis. *Immunity* 2000;13(5):691-702.
- (11) Ulrike B, Caroline D, Frauke W, Rodriguez-Palmero M, Kurt W, Reinhard P, et al. Activated T cells enter rat lymph nodes and Peyer's patches via high endothelial venules: survival by tissue-specific proliferation and preferential exit of CD8+ T cell progeny. *Eur J Immunol* 2006;29(5):1487-1495.

- (12) Bode U, Sparmann G, Westermann J. Gut-derived effector T cells circulating in the blood of the rat: preferential re-distribution by TGF β -1 and IL-4 maintained proliferation. *Eur J Immunol* 2001;31(7):2116-2125.
- (13) Butcher EC, Williams M, Youngman K, Rott L, Briskin M. Lymphocyte Trafficking and Regional Immunity. *Advances in Immunology* 1999; 72:209-253.
- (14) Berlin C, Berg EL, Briskin MJ, Andrew DP, Kilshaw PJ, Holzmann B, et al. Alpha 4 beta 7 integrin mediates lymphocyte binding to the mucosal vascular addressin MAdCAM-1. *Cell* 1993 July 16;74(1):185-195.
- (15) Norbert W, Löhler J, Tedder TF, Klaus R, Müller Werner, Steeber DA. L-selectin and β 7 integrin synergistically mediate lymphocyte migration to mesenteric lymph nodes. *Eur J Immunol* 1998;28(11):3832-3839.
- (16) Campbell DJ, Butcher EC. Rapid acquisition of tissue-specific homing phenotypes by CD4(+) T cells activated in cutaneous or mucosal lymphoid tissues. *The Journal of experimental medicine* 2002 Jan 7;195(1):135-141.
- (17) Bowman EP, Kuklin NA, Youngman KR, Lazarus NH, Kunkel EJ, Pan J, et al. The Intestinal Chemokine Thymus-expressed Chemokine (CCL25) Attracts IgA Antibody-secreting Cells. *Journal of Experimental Medicine* 2002 Jan 21;195(2):269-275.
- (18) Yoshida H, Naito A, Inoue J, Satoh M, Santee-Cooper SM, Ware CF, et al. Different Cytokines Induce Surface Lymphotoxin- $\alpha\beta$ on IL-7 Receptor- α Cells that Differentially Engender Lymph Nodes and Peyer's Patches. *Immunity* 2002;17(6):823-833.
- (19) GI microbiota and regulation of the immune system. New York; Austin, Tex.: Springer Science+Business Media; Landes Bioscience; 2008.
- (20) Ammann AJ, Hong R. Selective IgA deficiency: presentation of 30 cases and a review of the literature. *Medicine* 1971 May;50(3):223.
- (21) Yuki A, Hajime I, Saburo S, Chun YW, Eiichiro F, Masaru M, et al. Development of ulcerative colitis during the course of rheumatoid arthritis: Association with selective IgA deficiency. *World J Gastroenterol* 2006;12(32):5240-5243.
- (22) Mowat A. The anatomical basis of mucosal immune response. *Immunological Reviews* 1997(156):145-166.
- (23) Immune mechanisms in inflammatory bowel disease electronic resource. New York, N.Y.; Georgetown, Tex.: Springer Science+Business Media; Eureka.com/Landes Bioscience; 2006.
- (24) Tsuneyasu K, Shizuo A. Regulation of Dendritic Cell Function Through Toll-like Receptors. *Current Molecular Medicine* 2003 Jun;3(4):373-385.

- (25) Honda K, Sakaguchi S, Nakajima C, Watanabe A, Yanai H, Matsumoto M, et al. Selective Contribution of IFN- α/β Signaling to the Maturation of Dendritic Cells Induced by Double-Stranded RNA or Viral Infection. *Proceedings of the National Academy of Sciences of the United States of America* 2003 Sep 16;100(19):10872-10877.
- (26) Rescigno M, Urbano M, Valzasina B, Francolini M, Rotta G, Bonasio R, et al. Dendritic cells express tight junction proteins and penetrate gut epithelial monolayers to sample bacteria. *Nat Immunol* 2001;2(4):361-7.
- (27) van de Wal Y, Corazza N, Allez M, Mayer LF, Iijima H, Ryan M, et al. Delineation of a CD1d-restricted antigen presentation pathway associated with human and mouse intestinal epithelial cells. *Gastroenterology* 2003;124(5):1420-1431.
- (28) Hershberg RM, Mayer LF. Antigen processing and presentation by intestinal epithelial cells – polarity and complexity. *Immunology Today* 2000;21(3):123-128.
- (29) Sartor RB. Mechanisms of Disease: pathogenesis of Crohn's disease and ulcerative colitis. *Nature Clinical Practice Gastroenterology & Hepatology* 2006;3(7):390-407.
- (30) Katz KD. Intestinal permeability in patients with Crohn's disease and their healthy relatives. *Gastroenterology* 1989;97(4):927-931.
- (31) Teahon K, Smethurst P, Levi AJ, Menzies IS, Bjarnason I. Intestinal permeability in patients with Crohn's disease and their first-degree relatives. *Gut* 1992 Mar;33(3):320-323.
- (32) Hollander D. Permeability in Crohn's disease: altered barrier functions in healthy relatives? *Gastroenterology* 1993 June 01;104(6):1848-1851.
- (33) May GR, Sutherland LR, Meddings JB. Is small intestinal permeability really increased in relatives of patients with Crohn's disease? *Gastroenterology* 1993 June 01;104(6):1627-1632.
- (34) Yacyshyn BR, Meddings JB. CD45RO expression on circulating CD19+ B cells in Crohn's disease correlates with intestinal permeability. *Gastroenterology* 1995 January 01;108(1):132-137.
- (35) Peeters M, Geypens B, Claus D, Nevens H, Ghoo Y, Verbeke G, et al. Clustering of increased small intestinal permeability in families with Crohn's disease. *Gastroenterology* 1997 September 01;113(3):802-807.
- (36) Soderholm JD, Olaison G, Lindberg E, Hannestad U, Vindels A, Tysk C, et al. Different intestinal permeability patterns in relatives and spouses of patients with Crohn's disease: an inherited defect in mucosal defence? *Gut* 1999 January 01;44(1):96-100.

- (37) Wyatt J, Vogelsang H, Hubl W, Waldhoer T, Lochs H. Intestinal permeability and the prediction of relapse in Crohn's disease. *Lancet* 1993 June 05;341(8858):1437-1439.
- (38) Porter EM, Bevins CL, Ghosh D, Ganz T. The multifaceted Paneth Cell. *Cell Mol Life Sci* 2002 January 01;59(1):156-170.
- (39) Ouellette AJ. Paneth cells and innate mucosal immunity. *Curr Opin Gastroenterol* 2010 November 01;26(6):547-553.
- (40) Stappenbeck TS. Paneth Cell Development, Differentiation, and Function: New Molecular Cues. *Gastroenterology* 2009;137(1):30-33.
- (41) Strugnell RA, Wijburg OL. The role of secretory antibodies in infection immunity. *Nat Rev Microbiol* 2010 September 01;8(9):656-667.
- (42) Einerhand AW, Renes IB, Makkink MK, van der Sluis M, Buller HA, Dekker J. Role of mucins in inflammatory bowel disease: important lessons from experimental models. *Eur J Gastroenterol Hepatol* 2002 July 01;14(7):757-765.
- (43) Buisine MP, Desreumaux P, Leteurtre E, Copin MC, Colombel JF, Porchet N, et al. Mucin gene expression in intestinal epithelial cells in Crohn's disease. *Gut* 2001 October 01;49(4):544-551.
- (44) Molecular structure and function of the tight junction: from basic mechanisms to clinical manifestations. Boston, Mass.: Published by Blackwell Pub. on behalf of the New York Academy of Sciences; 2009.
- (45) Clayburgh DR, Shen L, Turner JR. A porous defense: the leaky epithelial barrier in intestinal disease. *Lab Invest* 2004 March 01;84(3):282-291.
- (46) Schmitz H, Barmeyer C, Fromm M, Runkel N, Foss HD, Bentzel CJ, et al. Altered tight junction structure contributes to the impaired epithelial barrier function in ulcerative colitis. *Gastroenterology* 1999 February 01;116(2):301-309.
- (47) D'Inca R, Sturniolo GC, Martines D, Di Leo V, Cecchetto A, Venturi C, et al. Functional and morphological changes in small bowel of Crohn's disease patients. Influence of site of disease. *Dig Dis Sci* 1995 June 01;40(6):1388-1393.
- (48) Marin ML, Geller SA, Greenstein AJ, Marin RH, Gordon RE, Aufses AH. Ultrastructural pathology of Crohn's disease: correlated transmission electron microscopy, scanning electron microscopy, and freeze fracture studies. *Am J Gastroenterol* 1983 June 01;78(6):355-364.
- (49) Kucharzik T, Walsh SV, Chen J, Parkos CA, Nusrat A. Neutrophil Transmigration in Inflammatory Bowel Disease Is Associated with Differential Expression of Epithelial

- Intercellular Junction Proteins. *The American Journal of Pathology* 2001;159(6):2001-2009.
- (50) Nighot P, Young K, Nighot M, Rawat M, Sung EJ, Maharshak N, et al. Chloride Channel CIC-2 is a Key Factor in the Development of DSS-induced Murine Colitis. *Inflammatory Bowel Diseases* 2013 Dec 1;19(13):2867-2877.
- (51) Nilius B, Droogmans G. Amazing chloride channels: an overview. *Acta Physiol Scand* 2003;177(2):119-147.
- (52) Moeser AJ, Haskell MM, Shifflett DE, Little D, Schultz BD, Blikslager AT. CIC-2 chloride secretion mediates prostaglandin-induced recovery of barrier function in ischemia-injured porcine ileum. *Gastroenterology* 2004 September 01;127(3):802-815.
- (53) Nighot PK, Moeser AJ, Ryan KA, Ghashghaei T, Blikslager AT. CIC-2 is required for rapid restoration of epithelial tight junctions in ischemic-injured murine jejunum. *Experimental Cell Research* 2009;315(1):110-118.
- (54) Nighot PK, Blikslager AT. CIC-2 regulates mucosal barrier function associated with structural changes to the villus and epithelial tight junction. *American Journal of Physiology-Gastrointestinal and Liver Physiology* 2010;299(2): G456.
- (55) Nighot PK, Blikslager AT. Chloride channel CIC-2 modulates tight junction barrier function via intracellular trafficking of occludin. *Am J Physiol Cell Physiol* 2012 January 01;302(1):178.
- (56) Yap AS, Briehner WM, Gumbiner BM. Molecular and functional analysis of cadherin-based adherens junctions. *Annu Rev Cell Dev Biol* 1997; 13:119-46.
- (57) *Inflammatory bowel disease: genetics, barrier function, immunologic mechanisms, and microbial pathways*. Boston, Mass.: Published by Blackwell Pub. on behalf of the New York Academy of Sciences; 2006.
- (58) Gassler N, Rohr C, Schneider A, Kartenbeck J, Bach A, Obermüller N, et al. Inflammatory bowel disease is associated with changes of enterocytic junctions. *American Journal of Physiology-Gastrointestinal and Liver Physiology* 2001;281(1): G228.
- (59) Jankowski JA, Bedford FK, Boulton RA, Cruickshank N, Hall C, Elder J, et al. Alterations in classical cadherins associated with progression in ulcerative and Crohn's colitis. *Lab Invest* 1998 September 01;78(9):1155-1167.
- (60) Doğan A, Wang ZD, Spencer J. E-cadherin expression in intestinal epithelium. *Journal of clinical pathology* 1995 Feb;48(2):143-146.
- (61) Madara JL, Stafford J. Interferon-gamma directly affects barrier function of cultured intestinal epithelial monolayers. *J Clin Invest* 1989 February 01;83(2):724-727.

- (62) Youakim A, Ahdieh M. Interferon- γ decreases barrier function in T84 cells by reducing ZO-1 levels and disrupting apical actin. *American Journal of Physiology-Gastrointestinal and Liver Physiology* 1999;276(5): G1288.
- (63) Schmitz H, Fromm M, Bentzel CJ, Scholz P, Detjen K, Mankertz J, et al. Tumor necrosis factor-alpha (TNFalpha) regulates the epithelial barrier in the human intestinal cell line HT-29/B6. *J Cell Sci* 1999 January 01;112 (Pt 1):137-146.
- (64) Marano CW, Lewis SA, Garulacan LA, Soler AP, Mullin JM. Tumor necrosis factor-alpha increases sodium and chloride conductance across the tight junction of CACO-2 BBE, a human intestinal epithelial cell line. *J Membr Biol* 1998 February 01;161(3):263-274.
- (65) Bruewer M, Luegering A, Kucharzik T, Parkos CA, Madara JL, Hopkins AM, et al. Proinflammatory cytokines disrupt epithelial barrier function by apoptosis-independent mechanisms. *J Immunol* 2003 December 01;171(11):6164-6172.
- (66) Tavalali S, Schmitz H, Fromm M, Schulzke J, Mankertz J. Expression from the human occludin promoter is affected by tumor necrosis factor alpha and interferon gamma. *Gastroenterology* 2000;118(4, Part 1): A602.
- (67) Gitter AH, Kerstin B, Heinz S, Schulzke J, Bentzel CJ, Michael F. Epithelial Barrier Defects in HT-29/B6 Colonic Cell Monolayers Induced by Tumor Necrosis Factor- α . *Ann N Y Acad Sci* 2006;915(1):193-203.
- (68) Cho JH, Brant SR. Recent Insights into the Genetics of Inflammatory Bowel Disease. *Gastroenterology* 2011;140(6): 1712.e2.
- (69) Probert CS, Jayanthi V, Hughes AO, Thompson JR, Wicks AC, Mayberry JF. Prevalence and family risk of ulcerative colitis and Crohn's disease: an epidemiological study among Europeans and south Asians in Leicestershire. *Gut* 1993 November 01;34(11):1547-1551.
- (70) Gordon H, Trier Moller F, Andersen V, Harbord M. Heritability in Inflammatory Bowel Disease: From the First Twin Study to Genome-Wide Association Studies. *Inflammatory Bowel Diseases* 2015 Jun 1;21(6):1428-1434.
- (71) Cortes A, Brown MA. Promise and pitfalls of the ImmunoChip. *Arthritis Res Ther* 2011 February 01;13(1):101.
- (72) Jostins L, Ripke S, Weersma RK, Duerr RH, McGovern DP, Hui KY, et al. Host-microbe interactions have shaped the genetic architecture of inflammatory bowel disease. *Nature* 2012 November 01;491(7422):119-124.
- (73) Goyal N, Rana A, Ahlawat A, Bijjem KR, Kumar P. Animal models of inflammatory bowel disease: a review. *Inflammopharmacology* 2014 August 01;22(4):219-233.

- (74) Koleva PT, Valcheva RS, Sun X, Gänzle MG, Dieleman LA. Inulin and fructo-oligosaccharides have divergent effects on colitis and commensal microbiota in HLA-B27 transgenic rats. *British Journal of Nutrition* 2012 Mar 14;108(9):1-11.
- (75) Bryda EC. *The Mighty Mouse: The Impact of Rodents on Advances in Biomedical Research*. 2013 Jan 1.
- (76) Ihle JN. Cytokine receptor signalling. *Nature* 1995 Oct 19;377(6550):591-594.
- (77) O'Shea JJ, Murray PJ. Cytokine Signaling Modules in Inflammatory Responses. *Immunity* 2008 Apr 11;28(4):477-487.
- (78) Alex P, Zachos NC, Nguyen T, Gonzales L, Chen TE, Conklin LS, et al. Distinct cytokine patterns identified from multiplex profiles of murine DSS and TNBS-induced colitis. *Inflammatory bowel diseases* 2009 Mar 1;15(3):341-352.
- (79) Fuss IJ, Neurath M, Boirivant M, Klein JS, de la Motte C, Strong SA, et al. Disparate CD4+ lamina propria (LP) lymphokine secretion profiles in inflammatory bowel disease. Crohn's disease LP cells manifest increased secretion of IFN-gamma, whereas ulcerative colitis LP cells manifest increased secretion of IL-5. *The Journal of Immunology* 1996 Aug 1;157(3):1261.
- (80) Camoglio L, te Velde AA, Tigges AJ, Das PK, van Deventer SJ. Altered expression of interferon-gamma and interleukin-4 in inflammatory bowel disease. *Inflammatory bowel diseases* 1998;4(4):285-290.
- (81) Melgar S, Yeung M.M-W, Bas A, Forsberg G, Suhr O, Oberg A, et al. Over-expression of interleukin 10 in mucosal T cells of patients with active ulcerative colitis. *Clinical & Experimental Immunology* 2003;134(1):127-137.
- (82) Fuss IJ. Nonclassical CD1d-restricted NK T cells that produce IL-13 characterize an atypical Th2 response in ulcerative colitis. *Journal of Clinical Investigation* 2004 May 15;113(10):1490-1497.
- (83) Rana SV, Sharma S, Kaur J, Prasad KK, Sinha SK, Kochhar R, et al. Relationship of cytokines, oxidative stress and GI motility with bacterial overgrowth in ulcerative colitis patients. *Journal of Crohn's and Colitis* 2014 Aug 1;8(8):859-865.
- (84) Ellrichmann M, Wietzke-Braun P, Dhar S, Nikolaus S, Arlt A, Bethge J, et al. Endoscopic ultrasound of the colon for the differentiation of Crohn's disease and ulcerative colitis in comparison with healthy controls. *Alimentary Pharmacology & Therapeutics* 2014;39(8):823-833.
- (85) Fort MM, Lesley R, Davidson NJ, Menon S, Brombacher F, Leach MW, et al. IL-4 Exacerbates Disease in a Th1 Cell Transfer Model of Colitis. *The Journal of Immunology* 2001 Feb 15;166(4):2793-2800.

- (86) Dennis O Gor, Noel R Rose, Neil S Greenspan. TH1-TH2: a Procrustean paradigm. *Nature Immunology* 2003 Jun 1;4(6):503-505.
- (87) Tsukada Y, Nakamura T, Iimura M, Iizuka BE, Hayashi N. Cytokine profile in colonic mucosa of ulcerative colitis correlates with disease activity and response to granulocytapheresis. *American Journal of Gastroenterology* 2002;97(11):2820-2828.
- (88) Yen D, Cheung J, Scheerens H, Poulet F, McClanahan T, McKenzie B, et al. IL-23 is essential for T cell-mediated colitis and promotes inflammation via IL-17 and IL-6. *The Journal of clinical investigation* 2006;116(5):1310-1316.
- (89) Strober W, Fuss IJ, Blumberg RS. The immunology of mucosal models of inflammation. *Annual Review of Immunology* 2002 Jan 1;20(1):495-549.
- (90) Jurjus AR, Khoury NN, Reimund J. Animal models of inflammatory bowel disease. *Journal of Pharmacological and Toxicological Methods* 2004;50(2):81-92.
- (91) E Gaudio, G Taddei, A Vetusch, R Sferra, G Frieri, G Ricciardi, et al. Dextran sulfate sodium (DSS) colitis in rats: clinical, structural, and ultrastructural aspects. *Digestive diseases and sciences* 1999 Jul 1;44(7):1458-1475.
- (92) Perše M, Cerar, A. Dextran Sodium Sulphate Colitis Mouse Model: Traps and Tricks. *Journal of Biomedicine and Biotechnology* 2012; 718617-13.
- (93) Neurath MF, Fuss I, Kelsall BL, Stueber E, Strober W. Antibodies to interleukin 12 abrogate established experimental colitis in mice. *Journal of Experimental Medicine* 1995 Jan 1;182(5):1281-1290.
- (94) Mannon PJ, Fuss IJ, Mayer L, Elson CO, Sandborn WJ, Present D, et al. Anti-Interleukin-12 Antibody for Active Crohn's Disease. *The New England Journal of Medicine* 2004 Nov 11;351(20):2069-2079.
- (95) Neurath MF, Fuss IJ, Pearlstein GR, Strober W, Marth T, Jain A. Anti-interleukin 12 treatment regulates apoptosis of Th1 T cells in experimental colitis in mice. *Gastroenterology* 1999;117(5):1078-1088.
- (96) Neurath MF, Fuss I, Pasparakis M, Alexopoulou L, Haralambous S, Meyer zum Bueschenfelde K, et al. Predominant pathogenic role of tumor necrosis factor in experimental colitis in mice. *European journal of immunology* 1997 Jul 1;27(7):1743-1750.
- (97) Johansson MEV, Gustafsson JK, Holmén-Larsson J, Jabbar KS, Xia L, Xu H, et al. Bacteria penetrate the normally impenetrable inner colon mucus layer in both murine colitis models and patients with ulcerative colitis. *Gut* 2014 Feb;63(2):281-291.

- (98) Kiesler P, Fuss IJ, Strober W. Experimental Models of Inflammatory Bowel Diseases. *Cellular and Molecular Gastroenterology and Hepatology* 2015;1(2):154-170.
- (99) Kiesler P, Fuss IJ, Strober W. Experimental Models of Inflammatory Bowel Diseases. *Cellular and Molecular Gastroenterology and Hepatology* 2015 Mar;1(2):154-170.
- (100) Wirtz S, Neufert C, Weigmann B, Neurath MF. Chemically induced mouse models of intestinal inflammation. *Nat Protoc* 2007;2(3):541-546.
- (101) Okayasu I, Hatakeyama S, Yamada M, Ohkusa T, Inagaki Y, Nakaya R. A novel method in the induction of reliable experimental acute and chronic ulcerative colitis in mice. *Gastroenterology* 1990 Mar;98(3):694-702.
- (102) Poritz LS, Garver KI, Green C, Fitzpatrick L, Ruggiero F, Koltun WA., M.D. Loss of the Tight Junction Protein ZO-1 in Dextran Sulfate Sodium Induced Colitis. *Journal of Surgical Research* 2007;140(1):12-19.
- (103) Kim JJ, Shajib MS, Manocha MM, Khan WI. Investigating Intestinal Inflammation in DSS-induced Model of IBD. 2012 Feb 1.
- (104) Samak G, Chaudhry KK, Gangwar R, Narayanan D, Jaggar JH, Rao R. Calcium/Ask1/MKK7/JNK2/c-Src signalling cascade mediates disruption of intestinal epithelial tight junctions by dextran sulfate sodium. *The Biochemical journal* 2015 Feb 1;465(3):503-515.
- (105) Randhawa PK, Singh K, Singh N, Jaggi AS. A Review on Chemical-Induced Inflammatory Bowel Disease Models in Rodents. *The Korean Journal of Physiology & Pharmacology* 2014 Aug 1;18(4):279-288.
- (106) H S Cooper, S N Murthy, R S Shah, D J Sedergran. Clinicopathologic study of dextran sulfate sodium experimental murine colitis. *Laboratory investigation; a journal of technical methods and pathology* 1993 Aug 1;69(2):238-249.
- (107) Giner E, Recio M, Ríos J, Giner R. Oleuropein protects against dextran sodium sulfate-induced chronic colitis in mice. *Journal of natural products* 2013 Jun 28;76(6):1113-1120.
- (108) Eichele DD, Kharbanda KK. Dextran sodium sulfate colitis murine model: An indispensable tool for advancing our understanding of inflammatory bowel diseases pathogenesis. *World J Gastroenterol* 2017;23(33):6016-6029.
- (109) Neurath M, Fuss I, Strober W. TNBS-Colitis. *Int Rev Immunol* 2000;19(1):51-62.
- (110) Antoniou Efstathios, Margonis GA, Angelou A, Pikouli A, Argiri P, Karavokyros I, Papalois A, Pikoulis E. The TNBS-induced colitis animal model: An overview. *Annals of Medicine and Surgery* 2016; 11:9-15.

- (111) Ikeda M, Takeshima F, Isomoto H, Shikuwa S, Mizuta Y, Ozono Y, et al. Simvastatin Attenuates Trinitrobenzene Sulfonic Acid-Induced Colitis, but Not Oxazalone-Induced Colitis. *Dig Dis Sci* 2008 Jul;53(7):1869-1875.
- (112) Cheon GJ, Cui Y, Yeon D, Kwon S, Park B. Mechanisms of Motility Change on Trinitrobenzenesulfonic Acid-Induced Colonic Inflammation in Mice. *The Korean Journal of Physiology & Pharmacology* 2012 Dec 1;16(6):437-446.
- (113) Qin H, Wu J, Tong X, Sung J, Xu H, Bian Z. Systematic review of animal models of post-infectious/post-inflammatory irritable bowel syndrome. *J Gastroenterol* 2011 Feb;46(2):164-174.
- (114) Isik F, Tunali Akbay T, Yarat A, Genc Z, Pisiriciler R, Caliskan-Ak E, et al. Protective Effects of Black Cumin (*Nigella sativa*) Oil on TNBS-Induced Experimental Colitis in Rats. *Dig Dis Sci* 2011 Mar;56(3):721-730.
- (115) Bouma G, Strober W. The immunological and genetic basis of inflammatory bowel disease. *Nature Reviews Immunology* 2003;3(7):521-533.
- (116) Michael Mähler, Bristol IJ, Leiter EH, Workman AE, Birkenmeier EH, Elson CO, et al. Differential susceptibility of inbred mouse strains to dextran sulfate sodium-induced colitis. *American Journal of Physiology - Gastrointestinal and Liver Physiology* 1998 Mar 1;274(3):544-551.
- (117) Mähler M, Bristol IJ, Sundberg JP, Churchill GA, Birkenmeier EH, Elson CO, et al. Genetic Analysis of Susceptibility to Dextran Sulfate Sodium-Induced Colitis in Mice. *Genomics* 1999 Jan 15;55(2):147-156.
- (118) Scheiffele F, Fuss IJ. Induction of TNBS colitis in mice. *Current protocols in immunology* 2002 Aug 1; Chapter 15: Unit 15.19.
- (119) Melgar S, Karlsson A, Michaëlsson E. Acute colitis induced by dextran sulfate sodium progresses to chronicity in C57BL/6 but not in BALB/c mice: correlation between symptoms and inflammation. *American Journal of Physiology - Gastrointestinal and Liver Physiology* 2005 Jun 1;288(6):1328-1338.
- (120) Mizoguchi A. Animal Models of Inflammatory Bowel Disease. *Progress in Molecular Biology and Translational Science Netherlands*; 2012. p. 263-320.
- (121) Bouma G, Kaushiva A, Strober W. Experimental murine colitis is regulated by two genetic loci, including one on chromosome 11 that regulates IL-12 responses. *Gastroenterology* 2002 Aug;123(2):554-565.
- (122) Suzuki T. Regulation of intestinal epithelial permeability by tight junctions. *Cell Mol Life Sci* 2013 Feb;70(4):631-659.

- (123) Collins FL, Rios-Arce ND, Atkinson S, Bierhalter H, Schoenherr D, Bazil JN, et al. Temporal and regional intestinal changes in permeability, tight junction, and cytokine gene expression following ovariectomy-induced estrogen deficiency. *Physiological Reports* 2017 May;5(9): n/a.
- (124) Low D, Nguyen DD, Mizoguchi E. Animal models of ulcerative colitis and their application in drug research. *Drug design, development and therapy* 2013;7:1341-1357.

CHAPTER 2

EFFECT OF GENETIC BACKGROUND ON INTESTINAL PERMEABILITY IN DSS AND TNBS-INDUCED COLITIS MODELS OF INFLAMMATORY BOWEL DISEASE

Shante S. Bryant¹, Anthony T. Blikslager², David W. Threadgill³

¹Department of Biological Sciences, Genetics Program, North Carolina State University,
²Department of Clinical Sciences, North Carolina State University, Raleigh, North Carolina,
³Department of Molecular and Cellular Medicine, Texas A&M Health Science Center

Abstract

Inflammatory Bowel Disease (IBD) represents a heterogeneous group of diseases, ulcerative colitis (UC) and Crohn's disease (CD), that are characterized by chronic intestinal inflammation. IBD results from an aberrant immune response to either pathogenic or resident luminal bacteria due to endogenous immunological or epithelial defects that perturb the normal tolerogenic response of the mucosal immune system. Experimentally-induced colitis in animal models has provided extensive insight into the complex mechanisms at work in the genesis of intestinal inflammation and the pathogenesis of IBD. The importance of gut bacteria in the etiology of IBD draws particular attention to the role played by intestinal epithelial cells and their ability to maintain the structure and function of the intestinal barrier. Increased intestinal permeability has been associated with clinical manifestations of colonic inflammation in human patients and in murine colitis models. Differential susceptibility to experimentally-induced intestinal inflammation has long been identified among several inbred mouse strains. We investigated the contrasting responses of C57BL/6 and BALB/c mice under two frequently utilized chemical models of inflammation. We hypothesized that differential susceptibility or resistance between these strains may be in part due to variations in the ability to maintain the epithelial barrier. No baseline difference in intestinal permeability was detected when measured via *in vivo* and *ex vivo* permeability assays. However, a significant increase in permeability was observed in C57BL/6 mice when treated with dextran sulfate sodium (DSS). Increased permeability persisted for up to 14 days after histopathological resolution of inflammation. In contrast to the DSS model, there was no observable shift in permeability in susceptible BALB/c mice when 2,4,6-trinitrobenzene sulfonic acid (TNBS) was administered intrarectally. These

results emphasize the effect of genetic background on the mechanistic pathways at work in experimentally-induced colitis in various animal models.

Introduction

Inflammatory bowel disease (IBD) commonly refers to two distinct conditions that involve chronic and relapsing inflammation of the intestines: ulcerative colitis (UC) and Crohn's disease (CD). IBD is more prevalent in developed countries, where as many as 1 out of 200 individuals are affected (1). Those suffering from IBD can often be difficult to diagnose and can present serious clinical challenges in terms of adequate treatment options for physicians. The etiology of IBD remains largely unknown, but clinical evidence supports a pathogenesis that involves complex interactions between genetic and internal environmental factors, particularly the microbiome (2-4). Because IBD is a multifactorial disease, understanding the underlying mechanisms is critically important for the development of more effective treatments and potential prevention strategies for predisposed individuals.

Genome-wide association studies (GWAS) have been successful in identifying genetic risk loci for both UC and CD and have even identified a subset of loci shared between the two conditions (5,6). Genes involved in several pathways that are crucial for intestinal homeostasis including barrier function, epithelial restitution, microbial defense, innate immune regulation, and adaptive immunity have been implicated through GWAS (7).

Animal models of IBD have been used for validation of candidate loci implicated in human studies as well as discovery of additional loci that may be involved in IBD pathogenesis. Several different animal models of IBD have been established to assist with defining the mechanisms of mucosal injury, inflammation, and repair. These models can be broadly divided into several categories including spontaneous colitis models, inducible colitis models, genetically-modified models, and adoptive transfer models (8-10). Although these models do not fully replicate the presentation of human disease, they are valuable tools that provide the means

to investigate the contribution of factors thought to be involved in the pathogenesis of IBD and the efficacy of different therapeutic options. In particular, chemically-induced murine models of intestinal inflammation are amongst the most commonly used, in part because they are relatively simple to induce and are highly repeatable. These models include dextran sulphate sodium (DSS)- and 2,4,6-trinitrobenzene sulfonic acid (TNBS)-induced colitis. However, similar to IBD itself, these chemically-induced models are poorly understood, particularly with regard to the apparent genetic predisposition of specific strains of mice to each of the chemicals.

Two strains of particular interest are C57BL/6 and BALB/c mice. These strains have contrasting responses to DSS and TNBS colitis induction, with C57BL/6 mice being highly susceptible to DSS but resistant to TNBS-induced colitis, whereas BALB/c mice are highly susceptible to TNBS but resistant to DSS-induced colitis. However, to our knowledge, the genetic mechanisms underlying these differences have not been studied and could be instructive in terms of human genetic predisposition to IBD.

Since our lab previously showed that mice with a mutation in the ion transporter *Clcn2* gene have compromised intestinal barrier function, resulting in increased disease severity when DSS is administered (11), we chose to examine the effect of genetic background on intestinal permeability in the two widely utilized chemical models of IBD. Our results demonstrate an effect of genetic background on mucosal barrier maintenance in DSS-induced but not in TNBS-induced colitis.

In addition to the commonly used C57BL/6 and BALB/c strains, first filial generation (F1) hybrid mice, were tested for sensitivity to DSS and TNBS induced colitis. CB6F1/J mice demonstrated intermediate phenotypes for weight loss and/or disease severity scores in the two chemically-induced models of colitis.

Materials and Methods

Animals

Animal studies were approved by the Institutional Care and Use Committee of North Carolina State University. Female and male C57BL/6, BALB/c, and CB6F1/J mice were purchased from The Jackson Laboratory (Bar Harbor, ME USA). CB6F1/J hybrid mice are the offspring of a cross between BALB/cJ females and C57BL/6J males. All animals used were between 7-15 weeks old. Mice were acclimated for ≥ 1 week before entering experimental studies.

Induction of Colitis

DSS model

Mice received 2.5% DSS (molecular weight 40,000–50,000 daltons; Affmetrix USB; Cleveland, OH) in autoclaved drinking water for 5 days as previously described [7]. For the recovery groups, DSS water was removed and mice were euthanized at 8, 12, and 19 days post initiation of DSS treatment.

TNBS model

A 2.5% TNBS solution was prepared by mixing 1 volume of 5% (w/v) Picrylsulfonic acid solution (TNBS; Sigma-Aldrich; MO, USA) with 1 volume of absolute ethanol (EtOH). Mice were lightly anesthetized with isoflurane. A 3.5 Fr umbilical catheter (Utah Medical Product, Inc., Utah, USA) was fitted to a 1 ml syringe and filled with the 2.5% TNBS solution. The catheter was lubricated and inserted 2 cm into the colon through the anus. 50 μ l of the TNBS solution was injected to slightly expand the colon. The catheter was then inserted another 2 cm into the colon where an additional 100 μ l of TNBS solution was administered, as previously described [7]. The mice were held in a vertical position for 1 minute after the intrarectal

injection. Control groups received a total of 150 μ l of 50% ethanol in a similar manner. TNBS treated and control mice were euthanized 3 days following administration of TNBS solution or 50% EtOH vehicle control respectively.

Assessment of Colitis

The clinical parameters recorded for each group were body weight, stool consistency, fecal blood, and diarrhea. The body weights of mice were monitored daily, and the disease activity index (DAI) score was assigned as summarized in Table 1. Scores for stool consistency and fecal blood were summed to give an overall DAI score. Mice that had weight loss greater than 20% were euthanized.

Histology

Tissues from colonic segments were collected and placed in 10% neutral buffered formalin for histological evaluation. Tissues were sectioned (5 μ m) and stained with hematoxylin and eosin.

Measurements of Barrier Integrity

Transepithelial Electrical Resistance

Colonic tissues were harvested immediately after euthanasia, cut longitudinally, and placed on 0.12-cm² aperture Ussing chambers. Tissues were bathed on the serosal and mucosal sides with murine Ringer's solution. The serosal bathing solution contained 10 mM glucose, which was osmotically balanced on the mucosal side with 10 mM mannitol. Bathing solutions were oxygenated (95% O₂-5% CO₂) and circulated in water-jacketed reservoirs maintained at 37°C. The spontaneous potential difference (PD) was measured with Ringer-agar bridges connected to calomel electrodes, and the PD was short circuited through Ag-AgCl electrodes with a voltage clamp that corrected for fluid resistance. Transepithelial electrical resistance

(TER, $\Omega \cdot \text{cm}^2$) was calculated from the spontaneous PD and short-circuit current. The Ussing chamber experiments were run for 60-min after an initial equilibration period of 15-min.

Paracellular Flux

To assess mucosal permeability, 0.2 $\mu\text{Ci/ml}$ [^3H]-mannitol was placed on the mucosal side of Ussing chamber-mounted tissues. After a 15-min equilibration period, standards were taken from the mucosal side of each chamber and a 60-min flux period was established by taking 0.5 ml samples from the serosal compartment. The presence of ^3H was established by measuring β -emission in a liquid scintillation counter (2900 TR Liquid Scintillation Analyzer, PerkinElmer). Unidirectional [^3H]-mannitol fluxes either from mucosa to serosa or from serosa to mucosa were evaluated by determining mannitol-specific activity added to the bathing solution on one side and calculating the net appearance of tritium over time in the bathing solution on other side, on a chamber unit area basis.

In vivo Intestinal Permeability Assay

In vivo intestinal permeability was assessed by gavage administration of FITC-dextran (4,000 daltons; Sigma-Aldrich, MO, USA), a non-metabolizable macromolecule that is used as a permeability probe. Food was withdrawn for 3 hr and mice were gavaged with FITC-dextran (6 mg/10 g body weight) 2 hr before euthanasia. Whole blood was collected by cardiac puncture at the time of euthanasia. Fluorescence intensity in serum was analyzed using a plate reader (excitation, 492 nm; emission, 525 nm).

Statistical Analysis

Analysis was performed with GraphPad Prism 7 for Mac OS X, Version 7.01 (La Jolla, CA) released April 02, 2016. Data are reported as mean \pm standard error. Whenever needed, data were analyzed by using an analysis of variance (Tukey's test was used for post-hoc analysis

between treatments after analysis of variance). $P < 0.05$ was considered significant for all analyses.

Results

DSS colitis severity is associated with genetic background

Body weight loss was observed from one day after removal of DSS (day 6) in C57BL/6 and peaked around day 8, with BALB/c mice experiencing little to no weight loss during DSS administration (Figure 2.1A). Through the recovery phase, C57BL/6 mice began to regain weight around day 10 but were unable to reach their starting baseline weight (Figure 2.1A). DAI scores showed that peak levels of diarrhea and fecal blood were found on day 5 in both strains (Figure 2.1B). Unlike BALB/c mice, which were able to fully recover, C57BL/6 mice exhibit a delayed recovery response with decreased weight and increased DAI that persisted for up to two weeks (day 19) after initial DSS administration. Furthermore, colon length decreased as disease progressed and was significantly shorter in both strains at day 8 (32% of baseline in C57BL/6 mice and 41% of baseline in BALB/c mice) (Figure 2.1C). In contrast to the C57BL/6 mice, CB6F1/J mice were similar to the BALB/c strain in that they experienced no significant weight loss over the course of DSS administration and recovery (Figure 2.1A). However, DAI scores for CB6F1/J mice fell in an intermediate range between the two parental strains (Figure 2.1B) and also exhibited a significant reduction in colon length at day 8 (11%) (Figure 2.1C).

Histopathological analysis was carried out using hematoxylin and eosin-stained sections of the distal colon (Figure 2.2). At day 8, all three strains showed loss of surface epithelium and infiltration of inflammatory cells into the mucosa (Figure 2.2D-F). These changes coincided with peak weight loss observed for all three genetic backgrounds (Figure 2.1A). Although, BALB/c mice did not experience significant weight loss or increased DAI, histological features were

similar to C57BL/6 mice and CB6F1/J mice at day 8. Re-epithelialization and restoration of tissue architecture was observed in all three strains by day 19, although C57BL/6 still showed residual clinical symptoms as reflected by their DAI score (Figure 2.1B and Figure 2.2G-I).

TNBS colitis severity shows different genetic background severity compared to DSS

Body weight loss was observed from day 1 in the BALB/c EtOH control group and in all groups exposed to TNBS (Figure 2.3A). Weight loss peaked at day 2 with TNBS-treated BALB/c mice losing a significant amount of weight in comparison to their respective EtOH treated counterparts (Figure 2.3A). Like with DSS responses, CB6F1/J also responded similarly to BALB/c upon TNBS exposure suggesting that the BALB/c background provides the dominant response alleles compared to C57BL/6. The BALB/c and CB6F1/J EtOH control groups did not experience any significant weight loss over the course of the study (Figure 2.3A). Animals were not recovered in the TNBS model, as with the DSS model, due to the significant weight loss (> 20%) experienced in the BALB/c and CB6F1/J TNBS-treated groups. DAI scores peaked at day 1 and consistently remained elevated in BALB/c and CB6F1/J mice treated with TNBS (Figure 2.3B). Conversely, symptoms in C57BL/6 mice had almost fully resolved by the completion of the study on day 3 despite experiencing a small peak in disease activity at day 1 (Figure 2.3B). No significant reduction in colon length was observed between EtOH and TNBS treated mice for any strain (Figure 2.3C).

Histological analysis was also performed using hematoxylin and eosin-stained sections of the distal colon (Figure 2.4). Because TNBS recapitulates the typical skip lesions seen in human CD, we examined longitudinal sections to account for this more ‘patchy’ distribution of inflamed tissue segments. Similar to the DSS model, all three strains showed loss of surface epithelium and infiltration of inflammatory cells into the mucosa when exposed to TNBS (Figure 2.4D-F).

However, in contrast to the BALB/c and CB6F1/J EtOH-treated animals, the C57BL/6 EtOH group also experienced epithelial degradation and permeation of immune cells into the mucosal tissue (Figure 2.4A-C).

Genetic background had no effect on baseline intestinal barrier function

Because barrier function is a critical component of clinical and experimental colitis, we tested whether there are baseline differences in barrier function between the genetic backgrounds. This was investigated by mounting colonic tissues on Ussing chambers. The average TER in all three strains was consistently around $75 \Omega \cdot \text{cm}^2$ (Figure 2.5A). Similarly, the mucosal-to-serosal paracellular flux of mannitol was not found to be significantly different between strains (Figure 2.5B). Taken together, these data indicate that there is no baseline difference in the intestinal permeability between BALB/c, C57BL/6, and CB6F1/J mice, at least in the distal colon studied. These data suggested that subsequent changes in permeability in response to DSS or TNBS in mice strains are attributable to conditions imposed through experimental conditions.

Genetic background had no effect on baseline intestinal permeability but did after DSS exposure

To assess integrity of the intestinal barrier before and after induction of DSS colitis, we utilized an *in vivo* paracellular permeability assay that measured flux of 4 kDa FITC-dextran from the intestinal lumen into the blood. Similar to experiments utilizing Ussing chambers, control animals showed no difference in flux of FITC-dextran as indicated by little variation in the average fluorescence readings for these mice (Figure 2.6A). To allow for comparisons between strains after administration of DSS, absorbance readings for these groups were normalized to their respective control groups and the fold change in intestinal permeability after

DSS treatment is reported on a logarithmic scale (\log_2). In accordance with clinical findings (weight loss, DAI) and histological findings, C57BL/6 mice had a sustained increase in paracellular permeability during DSS administration lasting up to two weeks after removal of DSS from the drinking water (Figure 2.6B). BALB/c and CB6F1/J mice demonstrated no change in permeability over the course of DSS treatment or during recovery (Figure 2.6B). These results indicate the role of genetic background on epithelial barrier function during the progression of disease in susceptible DSS treated C57BL/6 mice.

TNBS colitis was not associated with changes in permeability

Similar to the DSS model, barrier integrity was also accessed via an *in vivo* paracellular flux permeability assay in the TNBS model. TNBS-treated permeability data was normalized to EtOH-treated control data. Unlike the increased permeability noted particularly in C57BL/6 mice exposed to DSS, C57BL/6, BALB/c, and CB6F1/J mice showed no significant changes in permeability after administration of TNBS (Figure 2.7). This may relate to the more ‘patchy’ distribution of lesions noted in this model, making it difficult to detect an overall change in permeability.

Discussion

Colitis is induced by addition of DSS, a sulfated polysaccharide, to the drinking water over the course of several days. Animals exposed to DSS may develop acute or chronic colitis depending on the molecular weight, concentration, duration, and frequency of DSS administration. Clinical and histopathological features of DSS-colitis reflect those seen in human UC patients. Validation studies using various therapeutic agents for human IBD have shown that DSS-induced colitis can be used as a relevant model for the translation of mouse data to human disease (12). DSS is toxic to colonic epithelial cells and causes defects in the epithelial barrier

integrity. These defects can increase colonic mucosal permeability, allowing permeation of large molecules such as DSS, luminal antigens, and microorganisms into the mucosa resulting in a marked inflammatory response.

Our findings from this study show significant differences in epithelial barrier function using the DSS model. Susceptible C57BL/6 mice demonstrated a marked increase in intestinal permeability that persisted for up to two weeks after removal of DSS from the drinking water. *In vivo* paracellular flux of FITC-dextran was highest on day 5 which corresponded with the peak DAI score for the C57BL/6 group. Resistant BALB/c mice showed no change in permeability over the course of DSS administration or the recovery period. The single layered intestinal epithelium is a physical and immunological barrier that prevents direct contact of the intestinal mucosa with the luminal microbiota. Because DSS is toxic to the epithelial cells lining the intestine, administration of DSS in susceptible strains disrupts this barrier allowing entry of luminal antigens and microorganisms which elicits an inflammatory response. It has been shown that acute DSS-induced colitis does not require the presence of T cells or B cells as SCID mice develop colitis when exposed to DSS (13) . Thus, it is possible that DSS colitis is primarily initiated via activation of the innate immune system in response to the entry of luminal bacteria after epithelial injury. Our Ussing chamber studies demonstrated no baseline difference in the intestinal permeability (TER or flux) in the distal colons of untreated BALB/c, C57BL/6, or CB6F1/J mice. Indicating that the genetic predisposition for development of inflammation in the DSS model does not appear to originate solely due to inherent barrier function disruptions in C57BL/6 mice.

Measurements of TER via Ussing chambers are used to assess the integrity of tight junctions (TJs), the apical-most constituent of the intercellular junctional complex, as they reflect

the degree to which ions traverse epithelial tissue with electrical resistance across the monolayer being representative of paracellular resistance (14). Additionally, the mucosal-to-serosal flux of labeled solutes (mannitol, dextran) that do not undergo transcellular transport can be used to probe the permeability of the paracellular pathway and provide quantifiable measurements of paracellular permeability (15).

TJs form intimate contacts to restrict the passive flow of molecules from the lumen into the underlying lamina propria. Tight junctions consist of transmembrane, cytoskeletal, and signaling proteins that participate in intricate interactions to regulate paracellular permeability. Findings from other groups have demonstrated the dynamic nature of several TJ proteins during DSS induced colitis. Loss of the peripheral membrane protein ZO-1 corresponds with significantly increased expression of proinflammatory cytokines (TNF- α , IL-1 β , IFN- γ , IL-10, and IL-12) in the colon as soon as day 1 of DSS treatment (16). In the acute phase of DSS colitis, the impairment of epithelial barrier function has been associated with loss and redistribution of several other TJ proteins such as occludin, and claudin-1, -3, -4, and -5 (17). Previously, our lab has demonstrated that colitis severity and intestinal permeability is increased in *Cln2* knockout mice (11). The CLCN2 chloride channel is known to modulate intestinal TJ barrier function, and oral administration of lubiprostone, a pharmaceutical CLCN2 activator, significantly reduced the severity of colitis and reduced intestinal permeability in both DSS and TNBS induced colitis (18). Additionally, preventive treatment with lubiprostone induced significant recovery of the expression and distribution of selected sealing tight junction proteins in mice with DSS-induced colitis (18). Because altered expression and distribution of TJ proteins has been reported in human IBD, it is plausible that regulation of the intestinal barrier at the level of the TJ could be a

mechanism employed by our BALB/c mice to protect against the toxic effects of DSS to intestinal epithelium.

The involvement of NOD2 (a key CD susceptibility gene) in the pathogenesis of TNBS-induced colitis has led to the use of TNBS as a relevant model of human CD (19). For induction of colitis, TNBS dissolved in ethanol is administered into the rectum with a medical-grade polyurethane catheter. Ethanol is used as a means to effectively disrupt the intestinal barrier allowing TNBS to serve as a hapten and elicit immunologic responses by rendering colonic proteins immunogenic to the host immune system. A single dose of TNBS can lead to the development of an excessive cell mediated immune response reflected by acute type 1 t helper cell (Th1) induced inflammation (20). The involvement of IL-12 and TNF- α as effector cytokines during this Th1 response has further validated this model as an appropriate recapitulation of human CD (20-24).

In contrast to the results from our DSS model, we were able to show that there is no significant change in epithelial barrier function as measured via paracellular flux of FITC-dextran after administration of TNBS or EtOH vehicle control in the susceptible BALB/c or resistant C57BL/6 mice. For induction of TNBS colitis, ethanol is used to disrupt the barrier allowing permeation of the TNBS molecules from the lumen into the lamina propria. Intestinal inflammation is induced by altering host proteins through the formation of covalent bonds with trinitrophenyl haptens of TNBS (20). These hapten modified self-antigens are recognized by the host immune system and contribute to acute intestinal inflammation resulting from an immune-mediated inflammatory response (20). During this acute inflammation, the primary immune response observed follows a pro-inflammatory Th1 profile, increasing the expression of IL-12, IFN- γ and TNF- α (25,26). This mechanism of action coupled with our data on barrier integrity

suggests that TNBS-induced colitis is primarily mediated by the adaptive immune system via T-cell activation.

A single layer of columnar epithelial cells serves as the interface between the external environment and the mucosal immune system. This selective barrier works to limit infiltration of antigens and other macromolecules while simultaneously allowing the immune system to sample the luminal contents for both commensal and pathogenic organisms. This “sampling” allows the immune system to generate tolerance for dietary antigens and commensal organisms or effectively mount a response against pathogenic invaders. Disruption of epithelial barrier function and increased intestinal permeability has been well documented in both UC and CD, the two major IBD conditions (27,28). Both chemically induced animal models examined in this study (DSS & TNBS) can also produce disturbances in barrier integrity.

We have proposed intestinal barrier control as a means for BALB/c mice to protect against DSS induced colitis. Barrier dysfunction is a potential stimulating factor for induction of colitis in DSS treated but not in TNBS treated animals. These strain differences establish that colitis is not simply due to chemical injury of the colonic mucosa but instead arises from a complex interplay between genetic variants, environmental triggers, microbial communities, and the immune system as seen in human IBD. Our results indicate these specific models of IBD are not interchangeable, and that the final pathway of inflammation likely arises from distinct defects within each model. This is similar to what was found in GWAS studies from human UC and CD patients with several risk loci being shared between the two conditions in addition to risk loci that are exclusive to each disease.

Follow up studies are needed to investigate the exact mechanism by which the epithelial barrier is regulated in BALB/c mice during DSS treatment and to determine if the alteration in

the intestinal barrier function is a primary necessity for development of inflammation or a secondary event resulting from the inflammatory response in susceptible C57BL/6 mice. Moreover, protection from or predisposition for developing colitis in either model is heavily influenced by genetic background. Our work also has posited that like human IBD, chemically induced colitis is also a multifactorial trait attributable to various associations of resistance and/or susceptibility genes. Experimentally-induced colitis in the DSS and TNBS models appears to be under independent genetic control with the BALB/c genome acting dominantly over the C57BL/6 genome in both models. This is evident in the grouping of CB6F1/J phenotypes with BALB/c mice in response to each chemical. Animal models of IBD have long been known to recapitulate the histopathological and morphological features of human disease, but more focus should be directed toward their ability to mirror the considerable genetic heterogeneity that distinguishes UC and CD. Advances in IBD genetics have indicated modifications in genes regulating mucosal barrier integrity, innate immune response, and microbial homeostasis leading to increased utilization of genetic testing to broadly characterize disease prognosis and predict responses to specific therapies (29) . Because no single risk allele is sufficient to produce disease, the identification of gene-gene associations which synergistically increase disease likelihood is of particular importance. These multigene interactions may be replicated in murine crosses to define pathogenesis and validate newly developed therapies. Although, animal models have not been able to duplicate exactly the pathological characteristics of UC or CD, they are indispensable tools for exploration and characterization of disease pathophysiology.

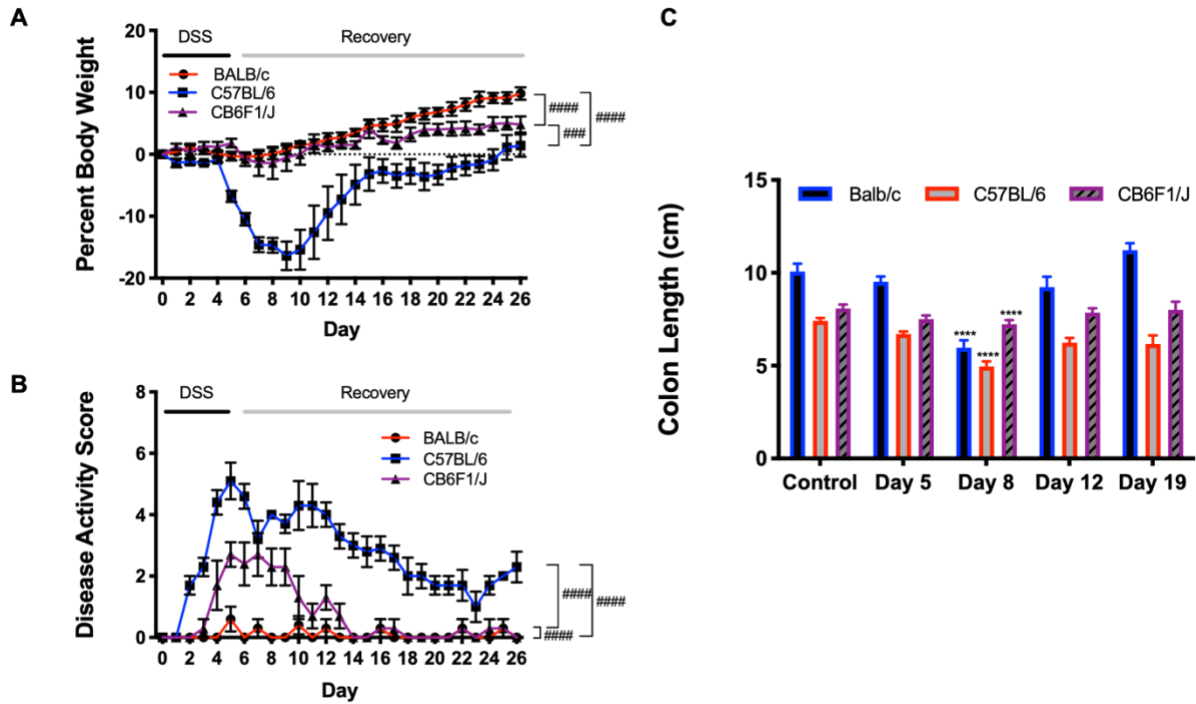


Figure 2.1. Severity of DSS colitis. (A) Body weight loss. (B) Disease activity score (DAI). (C) Colon length. The data are representative of more than 3 independent experiments (n=5-7 for each group in each experiment). Comparison to controls (*p<0.05, **p<0.01, ***p<0.001, ****p<0.0001). Comparisons between groups (#p<0.05, ##p<0.01, ###p<0.001, ####p<0.0001).

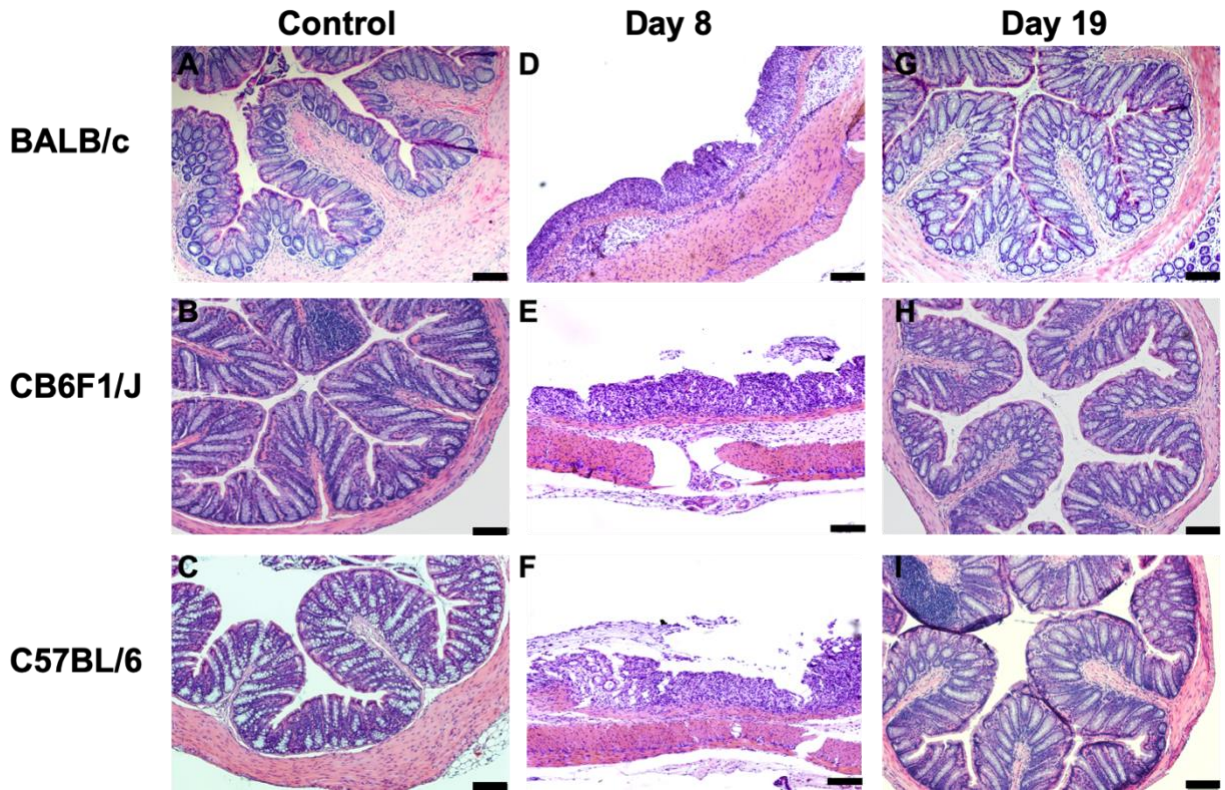


Figure 2.2. Distal colon histology in DSS colitis. BALB/c mice (A, D, G), CBF1/J mice (B, E, H), and C57BL/6 (C, F, I). Sections from control mice (A, B, C), mice that received DSS for 5 days and were recovered for 3 days (D, E, F), and mice that received DSS for 5 and were recovered for 14 additional days (G, H, I) Sections stained with hematoxylin-eosin. 4x magnification. Black bar = 100 μ m.

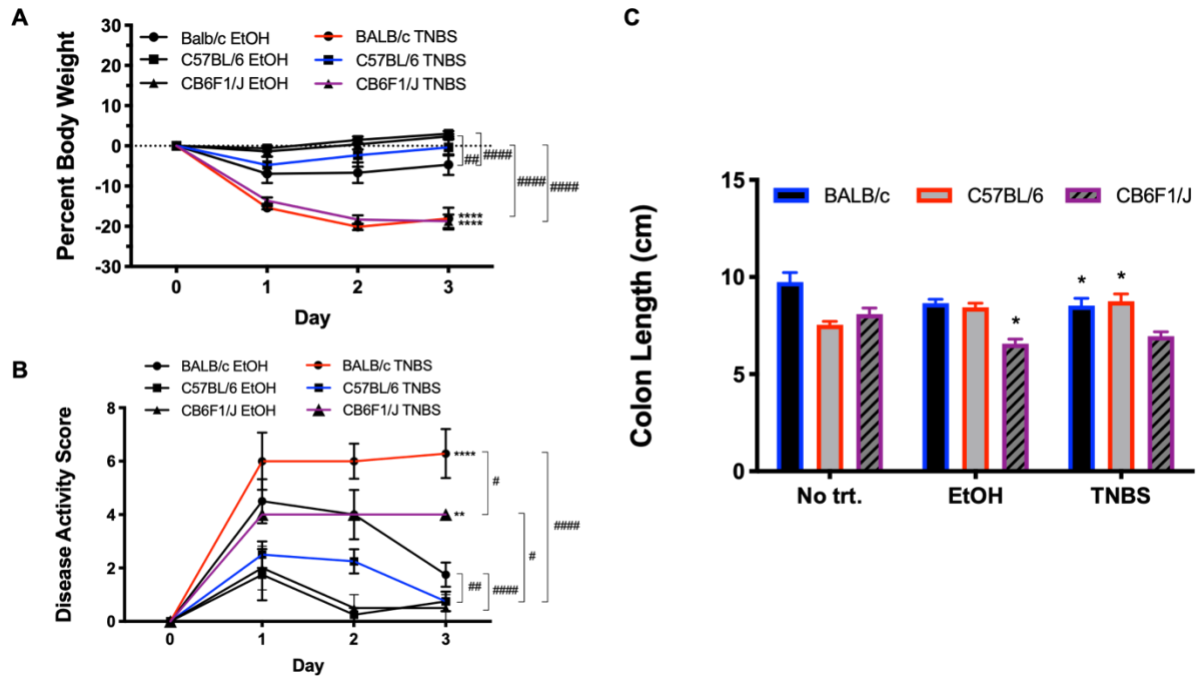


Figure 2.3. Severity of TNBS colitis. (A) Body weight loss. (B) Disease activity score (DAI). (C) Colon length. The data are representative of more than 3 independent experiments (n=4-8 for each group in each experiment). Comparison to controls (*p<0.05, **p<0.01, ***p<0.001, ****p<0.0001). Comparisons between groups (#p<0.05, ##p<0.01, ###p<0.001, ####p<0.0001).

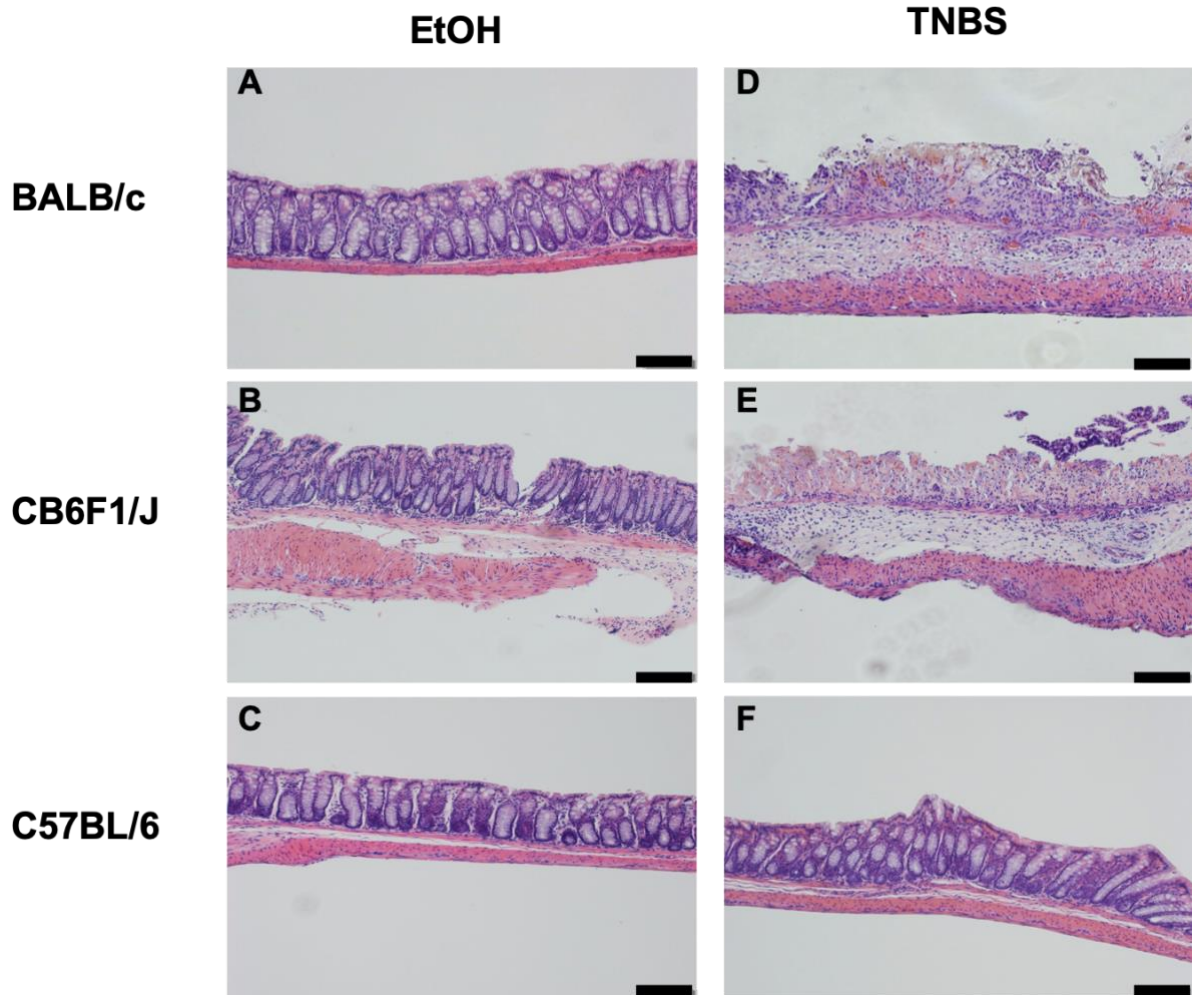


Figure 2.4 Distal colon histology in TNBS colitis. BALB/c mice (A and D), CB6F1/J mice (B and E), and C57BL/6 (C and F). Sections from EtOH treated control mice (A, B, C) and TNBS treated mice (D, E, F). Sections stained with hematoxylin-eosin. 4x magnification. Black bar = 100 μ m.

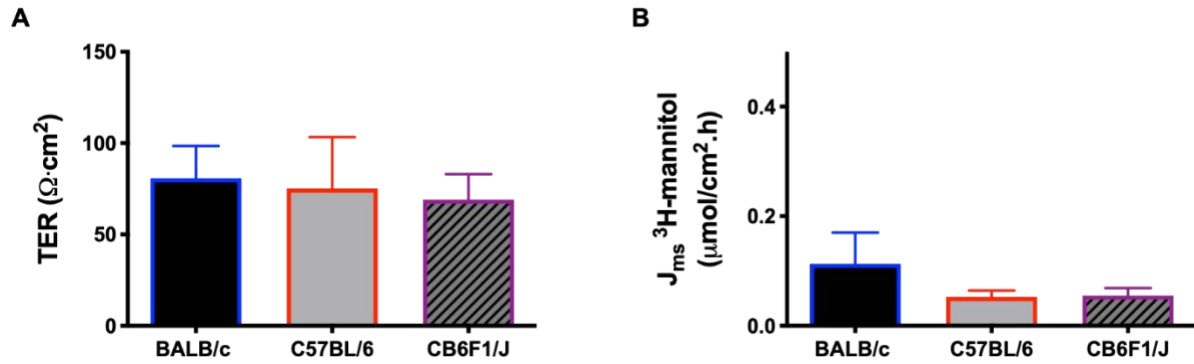


Figure 2.5. Baseline epithelial permeability. (A) In Ussing chambers experiments, there was no significant difference in transepithelial electrical resistance (TER) in the distal colons of BALB/c, C57BL/6, or CB6F1/J mice. (B) The mucosal-to-serosal paracellular flux of mannitol also showed no significant difference in the distal colons of BALB/c, C57BL/6, or CB6F1/J mice. (n=5-8 for each group).

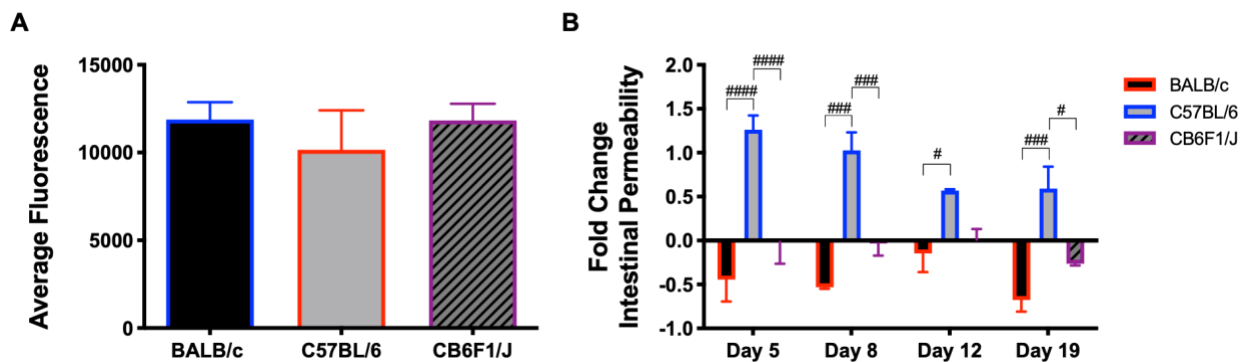


Figure 2.6. *In vivo* paracellular permeability for DSS colitis model. Evaluated by measuring flux of 4 kDa FITC-dextran. (A) Average fluorescence in untreated control mice (excitation, 492 nm; emission, 525 nm). (B) Fold change in permeability (normalized to controls) for DSS treated mice. Comparison to controls (*p<0.05, **p<0.01, ***p<0.001, ****p<0.0001). Comparisons between groups (#p<0.05, ##p<0.01, ###p<0.001, ####p<0.0001).

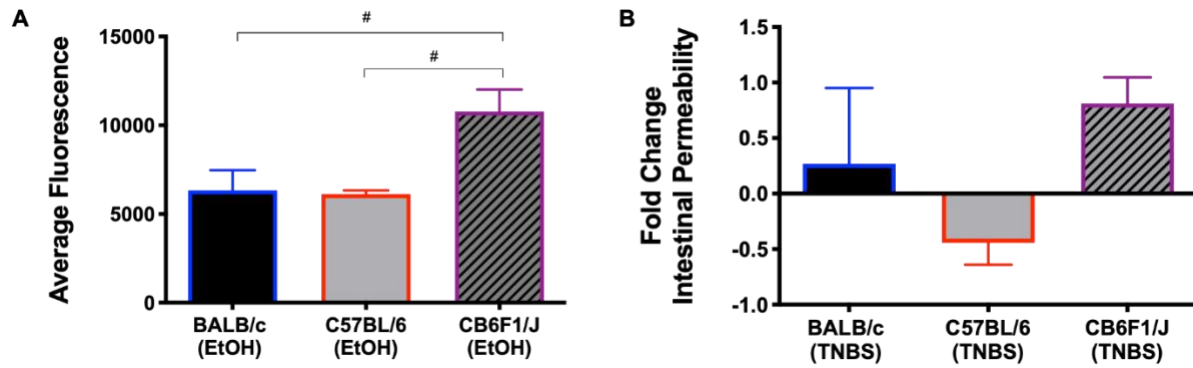


Figure 2.7. *In vivo* paracellular permeability for TNBS colitis model. Evaluated by measuring flux of 4 kDa FITC-dextran. (A) Average fluorescence in EtOH treated control mice (excitation, 492 nm; emission, 525 nm). (B) Fold change in permeability (normalized to controls) for TNBS treated mice. Comparison to controls (* $p < 0.05$, ** $p < 0.01$, *** $p < 0.001$, **** $p < 0.0001$). Comparisons between groups (# $p < 0.05$, ## $p < 0.01$, ### $p < 0.001$, #### $p < 0.0001$).

Table 2.1. Disease severity scoring system for DAI index. Scores reflect degree of weight loss, diarrhea, and visible fecal blood on a scale of 0-4. Scores are measured daily for each animal and added together to give an overall DAI measure for comparison.

Score	Weight Loss	Stool Consistency	Fecal Blood
0	<1%	Normal pellets	No blood
1	1-5%	Slightly loose feces	Slightly bloody
2	5-10%	Loose feces	Moderately bloody
3	10-15%	Feces sticks to anus	Gross bleeding
4	>15%	Watery diarrhea	Blood in entire colon

References

- (1) Gismera CS, Aladren BS. Inflammatory bowel diseases: a disease (s) of modern times? Is incidence still increasing? *World J Gastroenterol* 2008 September 28;14(36):5491-5498.
- (2) Sartor RB, Muehlbauer M. Microbial host interactions in IBD: implications for pathogenesis and therapy. *Curr Gastroenterol Rep* 2007 December 01;9(6):497-507.
- (3) Sartor RB. Microbial influences in inflammatory bowel diseases. *Gastroenterology* 2008 February 01;134(2):577-594.
- (4) Xavier RJ, Podolsky DK. Unravelling the pathogenesis of inflammatory bowel disease. *Nature* 2007 July 26;448(7152):427-434.
- (5) Franke A, McGovern DPB, Barrett JC, Wang K, Radford-Smith GL, Ahmad T, et al. Genome-wide meta-analysis increases to 71 the number of confirmed Crohn's disease susceptibility loci. *Nat Genet* 2010;42(12):1118-25.
- (6) Anderson CA, Boucher G, Lees CW, Franke A, D'Amato M, Taylor KD, et al. Meta-analysis identifies 29 additional ulcerative colitis risk loci, increasing the number of confirmed associations to 47. *Nat Genet* 2011;43(3):246-52.
- (7) Khor B, Gardet A, Xavier RJ. Genetics and pathogenesis of inflammatory bowel disease. *Nature* 2011;474(7351):307-17.
- (8) Neurath M, Fuss I, Strober W. TNBS-Colitis. *Int Rev Immunol* 2000;19(1):51-62.
- (9) Wirtz S, Neurath MF. Mouse models of inflammatory bowel disease. *Advanced Drug Delivery Reviews* 2007;59(11):1073-1083.
- (10) Wirtz S, Neufert C, Weigmann B, Neurath MF. Chemically induced mouse models of intestinal inflammation. *Nat Protoc* 2007;2(3):541-546.
- (11) Nighot P, Young K, Nighot M, Rawat M, Sung EJ, Maharshak N, et al. Chloride Channel ClC-2 is a Key Factor in the Development of DSS-induced Murine Colitis. *Inflammatory Bowel Diseases* 2013 Dec 1;19(13):2867-2877.
- (12) Melgar S, Karlsson L, Rehnström E, Karlsson A, Utkovic H, Jansson L, et al. Validation of murine dextran sulfate sodium-induced colitis using four therapeutic agents for human inflammatory bowel disease. *International Immunopharmacology* 2008;8(6):836-844.
- (13) Dieleman LA, Ridwan BU, Tennyson GS, Beagley KW, Bucy RP, Elson CO. Dextran sulfate sodium-induced colitis occurs in severe combined immunodeficient mice. *Gastroenterology* 1994 Dec;107(6):1643-1652.

- (14) Claude P. Morphological Factors Influencing Trans-Epithelial Permeability - Model for Resistance of Zonula-Occludens. *Journal of Membrane Biology* 1978;39(2-3):219-32.
- (15) Lane L. Clarke. A guide to Ussing chamber studies of mouse intestine. *American Journal of Physiology - Gastrointestinal and Liver Physiology* 2009 Jun;296(6):1151-1166.
- (16) Yan Y, Kolachala V, Dalmasso G, Nguyen H, Laroui H, Sitaraman SV, et al. Temporal and Spatial Analysis of Clinical and Molecular Parameters in Dextran Sodium Sulfate Induced Colitis. *PLoS One* 2009 Jun 1;4(6): 1e6073.
- (17) Poritz LS, Garver KI, Green C, Fitzpatrick L, Ruggiero F, Koltun WA. Loss of the Tight Junction Protein ZO-1 in Dextran Sulfate Sodium Induced Colitis. *Journal of Surgical Research* 2007;140(1):12-19.
- (18) Jin Y, Pridgen TA, Blikslager AT. Pharmaceutical Activation or Genetic Absence of ClC-2 Alters Tight Junctions During Experimental Colitis. *Inflammatory bowel diseases* 2015 Dec;21(12):2747-2757.
- (19) Watanabe T, Asano N, Murray PJ, Ozato K, Taylor P, Fuss IJ, et al. Muramyl dipeptide activation of nucleotide-binding oligomerization domain 2 protects mice from experimental colitis. *J Clin Invest* 2008;118(2):545-59.
- (20) Elson CO, Sartor RB, Tennyson GS, Riddell RH. Experimental models of inflammatory bowel disease. *Gastroenterology* 1995;109(4):1344-1367.
- (21) Morris GP, Beck PL, Herridge MS, Depew WT, Szewczuk MR, Wallace JL. Hapten-induced model of chronic inflammation and ulceration in the rat colon. *Gastroenterology* 1989 Mar;96(3):795-803.
- (22) Yu Q, Zhu S, Zhou R, Yi F, Bing Y, Huang S, et al. Effects of Sinomenine on the Expression of microRNA-155 in 2,4,6-Trinitrobenzenesulfonic Acid-Induced Colitis in Mice. *PLoS One* 2013 Sep 1;8(9): e73757.
- (23) Neurath MF, Fuss I, Kelsall BL, Stueber E, Strober W. Antibodies to interleukin 12 abrogate established experimental colitis in mice. *Journal of Experimental Medicine* 1995 Jan 1;182(5):1281-1290.
- (24) Boirivant M, Fuss IJ, Chu A, Strober W. Oxazolone Colitis: A Murine Model of T Helper Cell Type 2 Colitis Treatable with Antibodies to Interleukin 4. *Journal of Experimental Medicine* 1998 Nov 1;188(10):1929-1939.
- (25) Kawada M, Arihiro A, Mizoguchi E. Insights from advances in research of chemically induced experimental models of human inflammatory bowel disease. *World J Gastroenterol* 2007;13(42):5581-5593.

- (26) Fichtner-Feigl S, Fuss IJ, Young CA, Watanabe T, Geissler EK, Schlitt H, et al. Induction of IL-13 Triggers TGF-beta1-Dependent Tissue Fibrosis in Chronic 2,4,6-Trinitrobenzene Sulfonic Acid Colitis. *The Journal of Immunology* 2007 May 1;178(9):5859-5870.
- (27) Gitter AH, Wullstein F, Fromm M, Schulzke JD. Epithelial barrier defects in ulcerative colitis: characterization and quantification by electrophysiological imaging. *Gastroenterology* 2001 December 01;121(6):1320-1328.
- (28) Söderholm JD, Olaison G, Peterson KH, Franzén LE, Lindmark T, Wirén M, et al. Augmented increase in tight junction permeability by luminal stimuli in the non-inflamed ileum of Crohn's disease. *Gut* 2002 Mar;50(3):307-313.
- (29) Sartor RB. Mechanisms of Disease: pathogenesis of Crohn's disease and ulcerative colitis. *Nature Clinical Practice Gastroenterology & Hepatology* 2006 Jul;3(7):390-407.

CHAPTER 3

Genetic Analysis of DSS and TNBS-Induced Colitis on C57BL/6 and BALB/c Backgrounds

Shante S. Bryant¹, Anthony T. Blikslager², David W. Threadgill³

¹Department of Biological Sciences, Genetics Program, North Carolina State University,

²Department of Clinical Sciences, North Carolina State University, Raleigh, North Carolina,

³Department of Molecular and Cellular Medicine, Texas A&M Health Science Center

Abstract

The genetic basis for differential susceptibility of inbred mice to experimentally-induced colitis is unknown, particularly as it relates to comparison between different colitis models. Although several susceptibility loci for colitis have been identified, validation of proposed candidate genes is lacking and the mechanisms underlying inflammation remain poorly understood. To help elucidate the processes involved in the pathogenesis of intestinal inflammation, we compared the effect of genetic background on susceptibility to experimentally-induced colitis in two distinct mouse models (DSS and TNBS) of human inflammatory bowel disease (IBD). Mice from an F2 mapping population (F2CB) generated from parental BALB/c and C57BL/6 mice were phenotyped for disease severity based on percent body weight. QTL analysis did not reveal any significant QTL in either model, but suggestive regions were identified on chromosomes 6, 7, and 8 for the DSS model and on chromosome 2 for the TNBS model. We discuss potential approaches to increase our ability to detect significant QTL in our F2CB population, as well as, the use of combined QTL and transcriptome data to reduce the number of candidate genes that may be identified in our refined mapping analysis.

Introduction

Many disorders and common diseases in humans and animals with high prevalence, such as obesity (1), hypertension (2), Alzheimer's (3), and cancer (4) are inherited as complex traits. These diseases result from the interaction of environmental and genetic factors with phenotypic expression being influenced by multiple genes, which individually may increase or decrease the probability of disease development. Genetic determinants that are responsible for changes in the value of these traits are known as quantitative trait loci (QTLs) and are defined as a locus or haplotype whose variant alleles are associated with different average phenotypic values (5). Most quantitative traits are determined by several QTLs with a wide range of effect size that together control part of the phenotypic variation seen in a population (6). Environmental factors that modulate the biological effects of genetic factors coupled with epistatic interactions make it difficult to tease apart the individual effects of a specific locus on a particular phenotype(6). Thus, dissecting the genetic architecture of complex traits often requires a collaborative multi-disciplinary investigation and a variety of experimental approaches (7,8).

The ability to construct highly standardized and controlled conditions makes animal models a very effective means for investigating the genetic control of complex traits. Mouse models typically offer unparalleled opportunities for exploring the genetics of quantitative traits due to the availability of genomic sequence data for most commonly used strains and accessibility to a wide variety of strategies used to experimentally induce genetic alterations for validation of candidate genes of interest. Crosses of inbred strains with established phenotypic differences are typically used to examine gene–phenotype associations for the trait being studied (9). Backcrosses or F2 intercrosses bred from parental inbred strains are frequently utilized for identification of QTL in mice (10). Additionally, the existence of populations such as congenic

strains, recombinant inbred strains, or strains from the Collaborative Cross which are highly heterogeneous from a genetic standpoint provide exceptional tools for gene detection and the evaluation of allelic effects (10-12).

It is well accepted that inflammatory bowel disease (IBD) is a complex disorder characterized by chronic and relapsing inflammation of the digestive tract (13). Human genome-wide association studies (GWAS) have successfully identified genetic risk loci that are both specific to and have overlap in the two main conditions of IBD: ulcerative colitis (UC) and Crohn's disease (CD) (14). Furthermore, many IBD loci have been implicated in other immune-related disorders (ankylosing spondylitis, psoriasis)(13) and in infectious diseases of the gut (mycobacterial infection)(13,15). The basic etiology of IBD still remains largely unknown, but there are several factors such as dysregulation of innate and adaptive immune responses, disruptions in the structure and function of the intestinal barrier, and aberrant reactions to resident bacteria that have been implicated in the pathophysiology of these conditions (16).

Various experimental models of intestinal inflammation are available to help delineate the effects of these different etiological factors on the manifestation of this complex disease. These models represent a vital source of information about IBD pathogenesis that is clinically relevant to both UC and CD. Mouse models are among the most commonly used and include chemically-induced, spontaneous, genetically engineered, and transgenic models (16). Mice are a popular choice for studying intestinal injury and repair as mice have a gastrointestinal tract that is anatomically and functionally similar to that of humans (17). In addition, murine intestinal communities exhibit the same diversity of species (Firmicutes, Bacteroidetes, and Proteobacteria phyla) (18) and have many features analogous to the adaptive immune response seen in humans (19). Furthermore, comparative genomic studies have shown that up to 90% of human and

mouse genes are shared, with approximately 80% of mouse genes having a human orthologue (20,21).

Genetic differences in susceptibility to the development of experimentally-induced intestinal inflammation have long been identified among inbred strains of mice indicating a marked effect of genetic background on disease (22). Here we describe the use of a F2 mapping population (termed F2CB) to identify QTL that influence the development of colitis under two different chemically-induced models of IBD ((dextran sodium sulfate (DSS) and 2,4,6-trinitrobenzene sulfonic acid (TNBS)). The two parental strains used to generate the F2 population, BALB/c and C57BL/6, have opposing phenotypic responses to DSS and TNBS-induced colitis. BALB/c mice are highly susceptible to TNBS-induced colitis, while C57BL/6 mice develop minimal signs of colitis when TNBS is administered intrarectally. In contrast, C57BL/6 mice are highly susceptible to DSS-induced colitis, while BALB/c mice demonstrate a marked resistance to developing inflammation under this model. Although no statistically significant QTL regions were detected affecting inflammation in both models, several suggestive QTL were detected individually for DSS and TNBS-induced colitis suggesting that the two models of independent genetic susceptibilities supporting different underlying mechanisms of colitis.

Materials and Methods

Animals

Animal studies were approved by the Institutional Care and Use Committee of Texas A&M University. CB6F1/J hybrid mice which were the offspring of a cross between BALB/cJ females and C57BL/6J males were obtained from The Jackson Laboratory and were intercrossed to generate the F2 mapping population.

Induction of Colitis

DSS model

As described in chapter 2, mice received 2.5% DSS (molecular weight 40,000–50,000 daltons; Affmetrix USB; Cleveland, OH) in autoclaved drinking water for 5 days. Mice were euthanized at 8 days post initiation of DSS treatment or if body weight loss was greater than 20%.

TNBS model

As described in chapter 2, a 2.5% TNBS solution was prepared by mixing 1 volume of 5% (w/v) Picrylsulfonic acid solution (TNBS; Sigma-Aldrich; MO, USA) with 1 volume of absolute ethanol (EtOH). Mice were lightly anesthetized with isoflurane. A 3.5 Fr umbilical catheter (Utah Medical Product, Inc., Utah, USA) was fitted to a 1 ml syringe and filled with the 2.5% TNBS solution. The catheter was lubricated and inserted 2 cm into the colon through the anus. 50 μ l of the TNBS solution was injected to slightly expand the colon. The catheter was then inserted another 2 cm into the colon where an additional 100 μ l of TNBS solution was administered. The mice were held in a vertical position for 1 minute after the intrarectal injection. Mice were euthanized 3 days following administration of TNBS solution or if body weight loss was greater than 20%.

Phenotyping-Assessment of Colitis

The clinical parameters recorded for mice receiving DSS were body weight, stool consistency, fecal blood, and diarrhea. Body weight was the only parameter recorded for TNBS mice as they often did not produce stool that could be scored. The body weights of mice were monitored daily, and the disease activity index (DAI) score was assigned as summarized in

chapter 2, Table 1. Scores for stool consistency and fecal blood were summed to give an overall DAI score.

Genotyping

DNA extraction and genotyping from F2CB liver tissue was performed by GeneSeek (Neogen) using the Mouse Universal Genotyping Array (MUGA) on the Illumina Infinium platform (23). Genotypes were evaluated across 7851 SNP markers spaced uniformly every ~325 kb across the mouse reference genome (23).

QTL Mapping

QTL scans were performed with the scan1 function of R/qtl2 using a Haley Knott Regression. A permutation approach (n=1000) was used to generate genome-wide false discovery rate (FDR) thresholds for calculations of the LOD scores used to determine significance of each peak. 95% confidence intervals for the location of each peak were also established by the R/qtl2 program using the Bayesian credible interval.

Results

Phenotypic data was collected for a total of 203 F2CB mice between the two models (102 DSS mice, 101 TNBS mice). Of the initial cohort of mice, 101 mice from the DSS group and 82 mice from the TNBS group were used in the QTL analysis. Animals from the TNBS group experienced higher mortality associated with increased disease severity, and as a result 18 mice did not survive until the end of the study on day 3 post TNBS administration. Because of the typically poor condition of F2CB mice treated with TNBS, they often did not produce stool samples that could be scored for consistency and the presence of blood. Subsequently, these animals were only scored for percent body weight loss. Previous data from the two parental strains (C57BL/6 and BALB/c) used in the creation of the F2CB population display a strong

correlation between percent body weight and total disease severity which is summarized in the disease activity index (DAI) (Figure 3.1). The Pearson correlation coefficient (r) was calculated collectively from BALB/c, C57BL/6, and CB6F1/J mice for both DSS and TNBS ($r = -0.7853$ and $r = -0.7642$, respectively) indicating that percent body weight was an accurate predictor for disease severity (Figure 3.1).

Body weight data was collected on data from days 5 and 8 for the DSS model and on day 3 for the TNBS model. TNBS mice had the most drastic change in total percent body weight over the course of the study ($87\% \pm 0.7$), followed by DSS mice on day 8 ($93.3\% \pm 0.4$), and DSS mice on day 5 ($97.8\% \pm 0.4$) (Figure 3.2).

Two time points were evaluated for the DSS mice because overall DAI was highest on day 5 while body weight loss was greatest on day 8. QTL analysis was performed on percent body weight data as the phenotype of interest using the R/qtl2 software package with sex as a covariate. Although no statistically significant QTL were detected for either model, several suggestive QTL were identified for the individual models (Figures 3.3-3.5, Table 3.1). Two suggestive QTL, chromosome 8 for DSS and chromosome 2 for TNBS, are located near regions that harbor previously identified significant QTL with potential candidate genes related to the development of colitis in several animal models of IBD.

Discussion

It has been shown that acute inflammation in DSS converts to a predominantly Th-2 mediated response that morphologically and symptomatically resembles UC in humans (24-26). Whereas, TNBS colitis is characterized by a predominantly Th-1 immune response that presents with transmural inflammation that is typical of human CD (27,28). GWAS studies of both UC and CD have identified the presence of loci that are shared between the two conditions but also

the presence of regions that are exclusive to each disease type (29,30). Similarly, our QTL analysis suggests that the two models of human IBD are under independent genetic control that likely results in a final overall disease pathway. Although we were unable to detect statistically significant QTL from our F2CB mapping population, we were able to distinguish 5 suggestive QTL between the DSS and TNBS groups. Two QTL of particular interest that are located on chromosome 8 from the DSS analysis and on chromosome 2 from the TNBS analysis. Both QTL are located in regions that have previously been identified in QTL mapping experiments as being associated with intestinal inflammation in mice.

One of the first attempts to identify loci associated with susceptibility to experimentally-induced colitis was conducted using the DSS model. Segregating N2 and F2 populations generated from C3H/HeJ and C57BL/6J mice were phenotyped for the presence of histological lesions in the large intestine after administration of 3.5% DSS for 5 days (22). QTL screening identified five loci that significantly contributed to disease susceptibility, termed dextran sodium sulfate induced colitis (*Dssc*) (22). Two QTL, *Dssc1* on chromosome 5 (peak marker, 71.0 cM) and *Dssc2* on chromosome 2 (peak marker, 47.9 cM), were strongly associated with inflammation in the colon and accounted for 17.5% of the variance found in the colonic scoring (22).

Another QTL was also found on chromosome 2 in an F2 population created from IL10 deficient mice on C3H/HeJBir and C57BL/6 backgrounds (31). Susceptible IL10 deficient C3H/HeJBir mice develop spontaneous colitis and were phenotyped for colitis-related features such as spleen/body weight ratio, mesenteric lymph node/body weight ratio, and secretory IGA levels (31). Six major QTL contributing to colitis susceptibility as either main effectors and/or modifiers were identified in this analysis (31). The significant QTL, termed cytokine

deficiency-induced colitis 3 (*Cdcs3*), located on chromosome 2 (peak marker *D2Mit62*, 65 cM) was associated with hyperplasia and ulceration in the distal colon (31). Additionally, significant evidence for linkage for specific phenotypes associated with the inflammatory response of the cecum was detected on chromosome 8 (31). This QTL, termed *Cdcs4* (peak marker *D8Mit191*, 21 cM), appeared to influence other colitis related phenotypes through epistatic interactions with several *Cdcs* loci (31).

Furthermore, an additional locus on chromosome 2, glutathione peroxidase deficiency associated colitis 1 (*Gdac1*), that coincides with *Cdcs3* was found in a backcross mapping population generated from *Gpx1* and *Gpx2* double knockout (GPX1/2-DKO) mice (32). DKO mice on a mixed C57BL/6 and 129S1/SvimJ background exhibit spontaneous ileocolitis while DKO mice on a C57BL/6 only background exhibited a milder form of ileocolitis in comparison (32). Animals on a mixed B6;129 background were backcrossed to 129S1/SvimJ and analyzed for ileocolitis penetrance and severity at N5, N7, and N10 (32). Analysis of the C57BL/6 loci suggested a region of chromosome 2 as contributing to milder symptoms (32). A three-way comparison of nonsynonymous SNPs between 129S1/SvimJ, C57BL/6, and C3H/HeJBir mice pointed to seven major candidate genes (32), three of which are of particular interest here. The phospholipase A2 type IV genes (*Pla2g4b*, *Pla2g4e*, *Pla2g4f*) are involved in membrane remodeling and might play a role in epithelial restitution during the inflammatory response (33), making them appealing candidates for describing the significant difference seen in intestinal barrier integrity discussed in chapter 2.

Despite not being recapitulated in our analysis, two significant QTL (*Tnbs1* and *Tnbs2*) have been identified in the TNBS-colitis model from an F2 cross of highly susceptible SJL/J mice with resistant C57BL/6 mice (34) *Tnbs1* resides on chromosome 9 (46.41 cM) while *Tnbs2*

is found on chromosome 11 (20.62 cM) (34). The ability of susceptible SJL/J and resistant C57BL/6 mice to mount an IL12 response to bacterially derived lipopolysaccharide (LPS) demonstrated that SJL/J mice present with a markedly higher serum IL-12 response to LPS than resistant C57BL/6 mice (34). The gene for the IL12 p40 subunit was found within the *Tnbs2* region and was purported as a likely candidate for influencing susceptibility (34). IL12 is a known mediator for human CD (35) and has been implicated in experimentally-induced colitis (36).

Our analysis revealed the location of five suggestive QTL that were exclusive to each model. A suggestive QTL from the TNBS group found on chromosome 2 at 46.1 cM may likely coincide with the previously identified *Dssc2* locus (47.3 cM) and is located ~20 cM from the *Cdcs3* locus (65 cM). Furthermore, our suggestive QTL on chromosome 8 at 23.4 cM may be recapitulating the *Cdcs4* (21 cM) identified in the IL10 deficiency model. Other suggestive QTLs on chromosomes 6, 7, and 14 present novel regions not previously identified in experimentally-induced colitis models.

One of the key factors contributing to the success of a quantitative trait locus (QTL) mapping experiments is the precision with which QTL positions can be estimated. The precision of QTL can be affected by several factors which include the size and type of population used for mapping and the methods used for statistical analysis (37). Generally, QTL specificity should be greater with a larger population size (38). Because the accuracy with which a QTL can be mapped relative to a genetic marker is directly proportional to the number of recombination events between the marker and the trait locus (39), increasing our sample size would increase the number of recombinants in the interval being mapped, thereby increasing the likelihood of successfully identifying a significant QTL that is closely associated with our phenotype.

Additionally, choosing a genotyping platform with a higher density of markers would allow for higher resolution mapping of suggestive QTL. Later iterations of the MUGA (MegaMUGA-77,808 markers, GigaMUGA-143,259 markers) (23) exist that could prove useful for refining our mapping analysis.

Combinatorial approaches for dissecting the genetic architecture of complex traits/disease have been previously evaluated (40), demonstrating that understanding complex genetic traits often requires an integrative analysis. It has been proposed that the use of gene expression analysis from parental strains can accelerate the process of isolating individual genes found within identified QTL regions (40). Correlation of QTL data with transcriptional expression data from parental strains has proven successful in the identification of potential candidate genes in experimentally-induced mouse models of colitis (41,42). This combined methodology led to the identification of the vav guanine nucleotide exchange factor 3 (*Vav3*) gene as a candidate in *Trichuris muris*-induced chronic colitis (41). *Vav1/2/3* triple KO mice have been shown to have altered gut enterocyte differentiation/morphology and develop spontaneous colitis and ulceration in the cecum and ascending colon (43). Moreover, monocyte differentiation antigen which is produced by the (*Cd14*) gene has been associated with both CD (44) and UC (45) in humans and was also identified as a candidate from combined expression and QTL data in the IL10 deficient mouse model of colitis (42).

Because of the reported success of pooling expression and mapping data, we plan to perform RNA-sequencing to analyze differences in gene expression in our parental strains of mice (C57BL/6 and BALB/c) for both the DSS and TNBS models to help inform our QTL analysis. RNA-seq is a more appealing option over microarrays for several reasons: ability to detect novel transcripts (46,47), wider dynamic range (46-48), higher specificity and

sensitivity(49-51), and simple detection of rare and low-abundance transcripts. The considerably smaller sample size of sequencing just the parental strains instead of the entire F2CB population makes RNA-seq a feasible option from a cost perspective. It is our hope that this combinatorial approach should allow for the selection of a manageable number of candidates for future validation of their role in intestinal inflammation in both mice and humans.

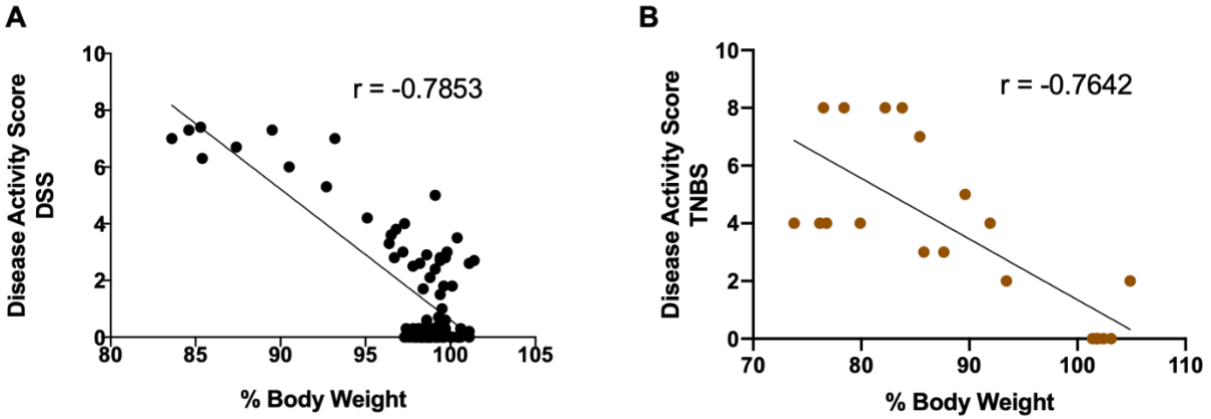


Figure 3.1. DAI and body weight correlation. (A) Correlation of DAI scores and percent body weight for DSS-induced colitis in susceptible C57BL/6 mice ($r = -0.8659$) (B) Correlation of DAI scores and percent body weight for TNBS-induced colitis in susceptible BALB/c mice ($r = -0.9605$).

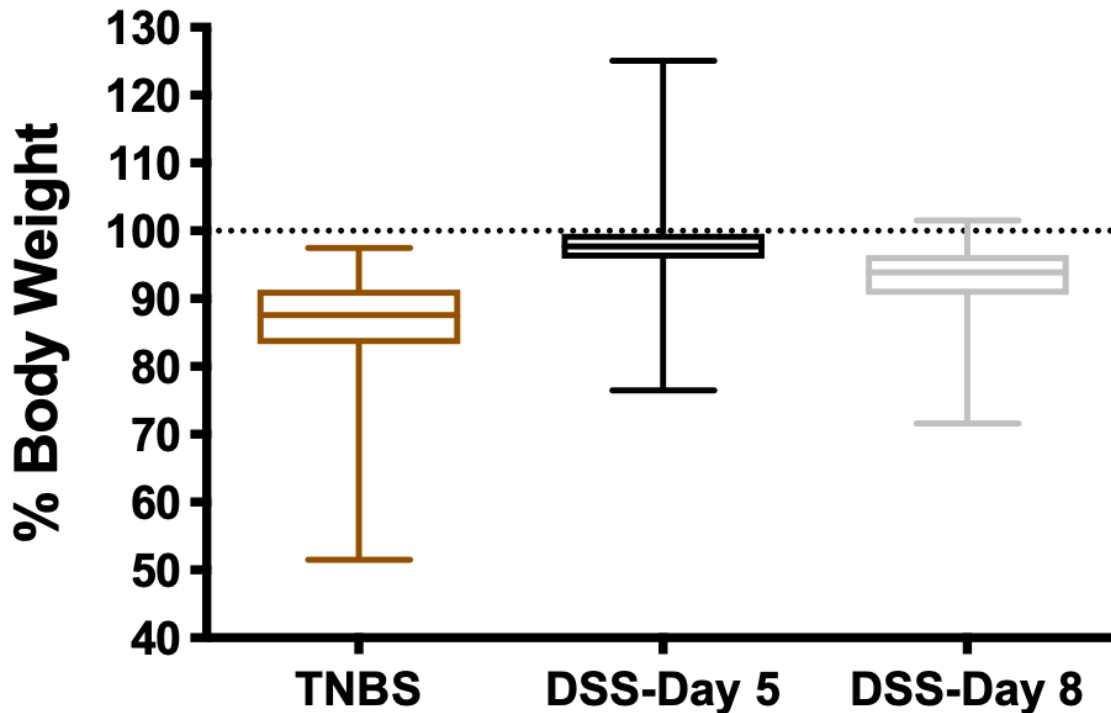


Figure 3.2. Percent body weight comparisons for F2CB mice. TNBS average percent body weight ($87\% \pm 0.7$), DSS-Day 5 average percent body weight ($97.8\% \pm 0.4$), DSS-Day 8 average percent body weight ($93.3\% \pm 0.4$).

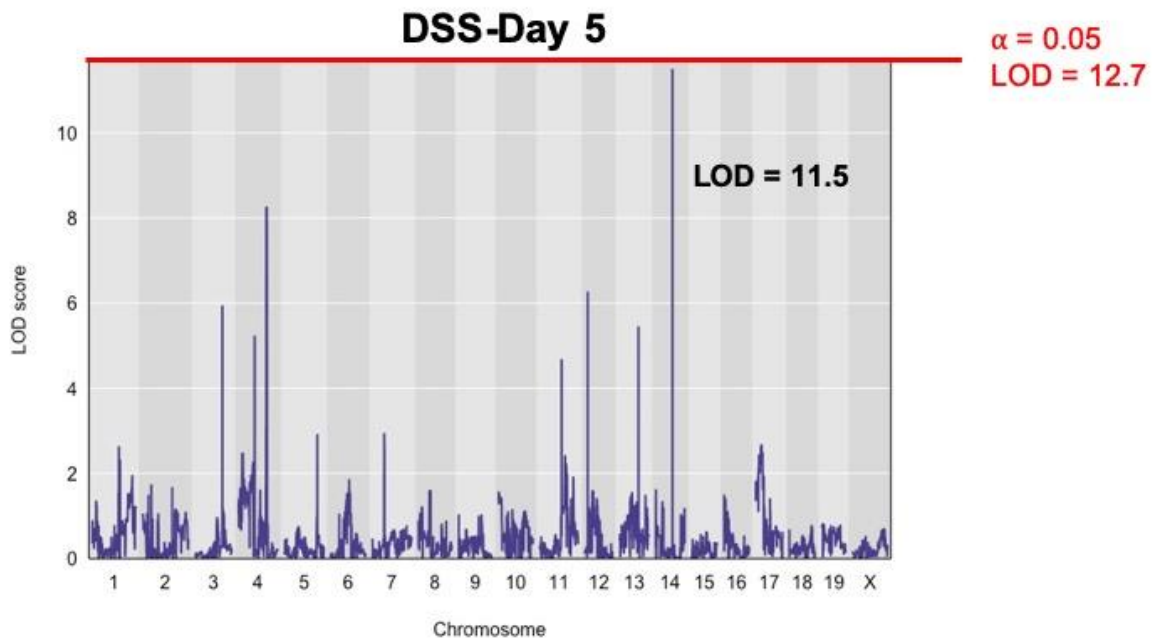


Figure 3.3. F2CB DSS day-5 QTL scan. Suggestive peak located on chromosome 14 (39.1 cM, LOD Score = 11.5).

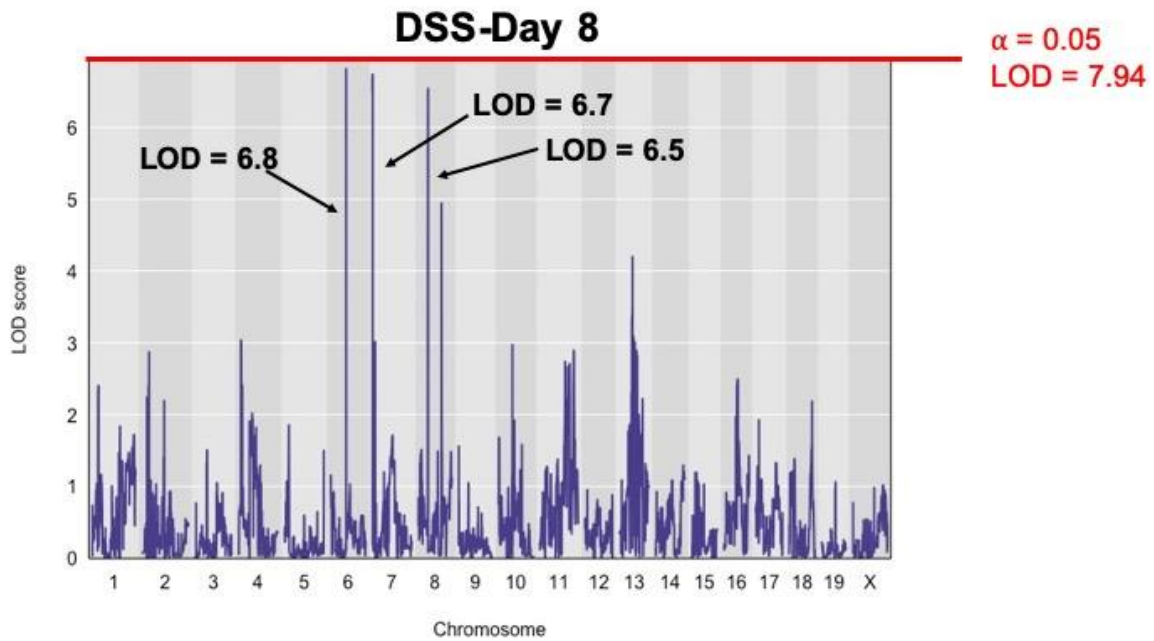


Figure 3.4. F2CB DSS day-8 QTL scan. Suggestive peak located on chromosome 6 (35.8 cM, LOD Score = 6.8). Suggestive peak located on chromosome 7 (2.4 cM, LOD Score = 6.7). Suggestive peak located on chromosome 8 (23.4cM, LOD Score = 6.5).

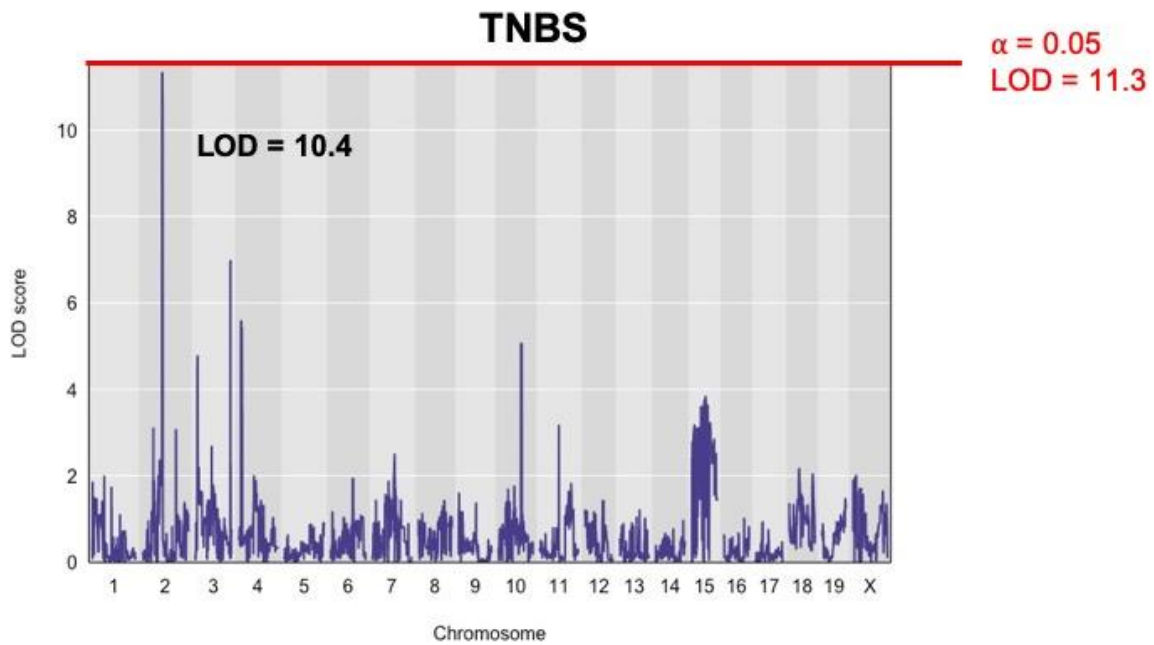


Figure 3.5. F2CB TNBS day-8 QTL scan. Suggestive peak located on chromosome 2 (46.1 cM, LOD Score = 10.4).

Table 3.1. Summary of suggestive QTL locations from F2CB mapping. Locations of suggestive QTL with respective LOD scores and significance thresholds.

Model (day)	Chromosome	Peak Position (cM)	CI-Lo (cM)	CI-Hi (cM)	LOD Score	α 0.2	α 0.05
TNBS	2	46.1	45.2	46.8	10.4	10.8	11.2
DSS (5)	14	39.1	39	39.2	11.5	12.1	12.7
DSS (8)	6	35.8	35.6	35.8	6.8	7.27	7.94
DSS (8)	7	2.4	1.9	2.7	6.7	7.27	7.94
DSS (8)	8	23.4	22.9	23.4	6.5	7.27	7.94

References

- (1) Burgess DJ. Complex traits: Old meets new in obesity genetics. *Nature reviews. Genetics* 2012 Apr 3;13(5):301.
- (2) O'Shaughnessy KM. Dissecting complex traits: recent advances in hypertension genomics. *Genome medicine* 2009 Apr 28;1(4):43.
- (3) Ridge PG, Mukherjee S, Crane PK, Kauwe JSK. Alzheimer's disease: analyzing the missing heritability. *PloS one* 2013;8(11): e79771.
- (4) Balmain A. Cancer as a Complex Genetic Trait: Tumor Susceptibility in Humans and Mouse Models. *Cell* 2002;108(2):145-152.
- (5) edited by SA. *Quantitative trait loci (QTL): methods and protocols*. New York: Humana Press/Springer, c2012; 2012.
- (6) Falconer DS, Mackay T. *Introduction to quantitative genetics*. Essex, England: Longman, 1996; 1996.
- (7) Stylianou IM, Affourtit JP, Shockley KR, Wilpan RY, Abdi FA, Bhardwaj S, et al. Applying Gene Expression, Proteomics and Single-Nucleotide Polymorphism Analysis for Complex Trait Gene Identification. *Genetics* 2008 Mar 1;178(3):1795-1805.
- (8) Holmberg J, Tordsson J, Holmdahl R, Olofsson P, Lu S, Åkerström B. Positional identification of *Ncf1* as a gene that regulates arthritis severity in rats. *Nature Genetics* 2003;33(1):25-32.
- (9) Mackay T. Quantitative trait loci in *Drosophila*. *Nature Reviews Genetics* 2001; 2:11-20.
- (10) Abiola O, Angel JM, Avner P, Bachmanov AA, Belknap JK, Bennett B, et al. The nature and identification of quantitative trait loci: a community's view. *Nature Reviews Genetics* 2003;4(11):911-916.
- (11) Bennett B, Beeson M, Gordon L, Carosone-Link P, Johnson TE. Genetic Dissection of Quantitative Trait Loci Specifying Sedative/Hypnotic Sensitivity to Ethanol: Mapping with Interval-Specific Congenic Recombinant Lines. *Alcoholism: Clinical and Experimental Research* 2002;26(11):1615-1624.
- (12) Aylor DL, Valdar W, Foulds-Mathes W, Buus RJ, Verdugo RA, Baric RS, et al. Genetic analysis of complex traits in the emerging Collaborative Cross. *Genome research* 2011;21(8):1213-1222.
- (13) Jostins L, Ripke S, Weersma RK, Duerr RH, McGovern DP, Hui KY, et al. Host-microbe interactions have shaped the genetic architecture of inflammatory bowel disease. *Nature* 2012;491(7422):119-124.

- (14) Khor B, Gardet A, Xavier RJ. Genetics and pathogenesis of inflammatory bowel disease. *Nature* 2011 Jun 16;474(7351):307-317.
- (15) Patel SY, Doffinger R, Barcenas-Morales G, Kumararatne DS. Genetically determined susceptibility to mycobacterial infection. *Journal of Clinical Pathology* 2008 Sep;61(9):1006-1012.
- (16) Goyal N, Rana A, Ahlawat A, Bijjem K, Kumar P. Animal models of inflammatory bowel disease: a review. *Inflammopharmacol* 2014 Aug;22(4):219-233.
- (17) Jiminez JA, Uwiera TC, Douglas Inglis G, Uwiera RR. Animal models to study acute and chronic intestinal inflammation in mammals. *Gut Pathogens* 2015 Jan 1;7(29):29.
- (18) Relman DA, McFall-Ngai M, Dethlefsen L. An ecological and evolutionary perspective on human-microbe mutualism and disease. *Nature* 2007 Oct 18;449(7164):811-818.
- (19) Mestas J, Hughes CCW. Of Mice and Not Men: Differences between Mouse and Human Immunology. *The Journal of Immunology* 2004 Mar 1;172(5):2731-2738.
- (20) Mouse Genome Sequencing Consortium, Waterson RH, Lindblad-Toh K, Birney E, Rogers J, Abril JF, et al. Initial sequencing and comparative analysis of the mouse genome. *Nature* 2002 Dec 5;420(6915):520-562.
- (21) Lin J, Hackam DJ. Worms, flies and four-legged friends: the applicability of biological models to the understanding of intestinal inflammatory diseases. *Disease models & mechanisms* 2011;4(4):447-456.
- (22) Mähler M, Bristol IJ, Sundberg JP, Churchill GA, Birkenmeier EH, Elson CO, et al. Genetic Analysis of Susceptibility to Dextran Sulfate Sodium-Induced Colitis in Mice. *Genomics* 1999 Jan 15;55(2):147-156.
- (23) Morgan AP, Fu C, Kao C, Welsh CE, Didion JP, Yadgary L, et al. The Mouse Universal Genotyping Array: From Substrains to Subspecies. *G3 (Bethesda, Md.)* 2015 Dec 18;6(2):263-279.
- (24) Alex P, Zachos NC, Nguyen T, Gonzales L, Chen TE, Conklin LS, et al. Distinct cytokine patterns identified from multiplex profiles of murine DSS and TNBS-induced colitis. *Inflammatory bowel diseases* 2009 Mar 1;15(3):341-352.
- (25) Jurjus AR, Khoury NN, Reimund J. Animal models of inflammatory bowel disease. *Journal of Pharmacological and Toxicological Methods* 2004;50(2):81-92.
- (26) E Gaudio, G Taddei, A Vetuschi, R Sferra, G Frieri, G Ricciardi, et al. Dextran sulfate sodium (DSS) colitis in rats: clinical, structural, and ultrastructural aspects. *Digestive diseases and sciences* 1999 Jul 1;44(7):1458-1475.

- (27) Neurath MF. Antibodies to interleukin 12 abrogate established experimental colitis in mice. *Journal of Experimental Medicine* 1995;182(5):1281-1290.
- (28) Mannon PJ, Fuss IJ, Mayer L, Elson CO, Sandborn WJ, Present D, et al. Anti-Interleukin-12 Antibody for Active Crohn's Disease. *The New England Journal of Medicine* 2004 Nov 11;351(20):2069-2079.
- (29) Franke A, McGovern DPB, Barrett JC, Wang K, Radford-Smith GL, Ahmad T, et al. Genome-wide meta-analysis increases to 71 the number of confirmed Crohn's disease susceptibility loci. *Nat Genet* 2010;42(12):1118-25.
- (30) Anderson CA, Boucher G, Lees CW, Franke A, D'Amato M, Taylor KD, et al. Meta-analysis identifies 29 additional ulcerative colitis risk loci, increasing the number of confirmed associations to 47. *Nat Genet* 2011;43(3):246-52.
- (31) Farmer MA, Sundberg JP, Bristol IJ, Churchill GA, Li R, Elson CO, et al. A Major Quantitative Trait Locus on Chromosome 3 Controls Colitis Severity in IL-10-Deficient Mice. *Proceedings of the National Academy of Sciences of the United States of America* 2001 Nov 20;98(24):13820-13825.
- (32) Esworthy RS, Kim B, Larson GP, Yip MLR, Smith DD, Li M, et al. Colitis locus on chromosome 2 impacting the severity of early-onset disease in mice deficient in GPX1 and GPX2. *Inflammatory Bowel Diseases* 2011;17(6):1373-1386.
- (33) Ghosh M, Tucker DE, Burchett SA, Leslie CC. Properties of the Group IV phospholipase A2 family. *Progress in lipid research* 2006;45(6):487-510.
- (34) Bouma G, Kaushiva A, Strober W. Experimental murine colitis is regulated by two genetic loci, including one on chromosome 11 that regulates IL-12 responses. *Gastroenterology* 2002;123(2):554-565.
- (35) Monteleone G, Biancone L, Marasco R, Marasco O, Morrone G, Luzzza F, et al. Interleukin 12 is expressed and actively released by Crohn's disease intestinal lamina propria mononuclear cells. *Gastroenterology* 1997;112(4):1169-1178.
- (36) Neurath MF. Antibodies to interleukin 12 abrogate established experimental colitis in mice. *Journal of Experimental Medicine* 1995;182(5):1281-1290.
- (37) Zeng ZB. Precision Mapping of Quantitative Trait Loci. *Genetics* 1994;136(4):1457-1468.
- (38) Yan J, Tang J, Meng Y, Ma X, Teng W, Chander S, et al. Improving QTL Mapping Resolution Based on Genotypic Sampling a Case Using a RIL Population. *Acta Genetica Sinica* 2006;33(7):617-624.
- (39) Mackay T. The genetic architecture of quantitative traits. *Annual Review of Genetics* 2001; 35:303-339.

- (40) Verdugo RA, Farber CR, Warden CH, Medrano JF. Serious limitations of the QTL/Microarray approach for QTL gene discovery. *BMC biology* 2010;8(1):96.
- (41) Levison SE, Fisher P, Hankinson J, Zeef L, Eyre S, Ollier WE, et al. Genetic analysis of the *Trichuris muris*-induced model of colitis reveals QTL overlap and a novel gene cluster for establishing colonic inflammation. *BMC genomics* 2013;14(1):127.
- (42) de Buhr MF, Mähler M, Geffers R, Hansen W, Westendorf AM, Lauber J, et al. *Cd14*, *Gbp1*, and *Pla2g2a*: three major candidate genes for experimental IBD identified by combining QTL and microarray analyses. *Physiological Genomics* 2006;25(3):426-434.
- (43) Liu JY, Seno H, Miletic AV, Mills JC, Swat W, Stappenbeck TS. Vav proteins are necessary for correct differentiation of mouse cecal and colonic enterocytes. *Journal of Cell Science* 2009 Feb 1;122(3):324-334.
- (44) Klein W, Tromm A, Griga T, Fricke H, Folwaczny C, Hocke M, et al. A Polymorphism in the *CD14* Gene is Associated with Crohn Disease. *Scandinavian Journal of Gastroenterology* 2002;37(2):189-191.
- (45) Obana N, Takahashi S, Kinouchi Y, Negoro K, Takagi S, Hiwatashi N, et al. Ulcerative Colitis is Associated with a Promoter Polymorphism of Lipopolysaccharide Receptor Gene, *CD14*. *Scandinavian Journal of Gastroenterology* 2002;37(6):699-704.
- (46) Snyder M, Wang Z, Gerstein M. RNA-Seq: a revolutionary tool for transcriptomics. *Nature Reviews Genetics* 2009;10(1):57-63.
- (47) Wilhelm BT, Landry J. RNA-Seq—quantitative measurement of expression through massively parallel RNA-sequencing. *Methods* 2009;48(3):249-257.
- (48) Zhao S, Fung-Leung W, Bittner A, Ngo K, Liu X. Comparison of RNA-Seq and Microarray in Transcriptome Profiling of Activated T Cells. *PloS one* 2014;9(1): e78644.
- (49) Wang C, Gong B, Bushel PR, Thierry-Mieg J, Thierry-Mieg D, Xu J, et al. The concordance between RNA-seq and microarray data depends on chemical treatment and transcript abundance. *Nature Biotechnology* 2014;32(9):926-932.
- (50) Li J, Hou R, Niu X, Liu R, Wang Q, Wang C, et al. Comparison of microarray and RNA-Seq analysis of mRNA expression in dermal mesenchymal stem cells. *Biotechnol Lett* 2016;38(1):33-41.
- (51) Liu Y, Morley M, Brandimarto J, Hannenhalli S, Hu Y, Ashley EA, et al. RNA-Seq identifies novel myocardial gene expression signatures of heart failure. *Genomics* 2015;105(2):83-89.

CHAPTER 4

Future Directions and Conclusions

Research Summary

The research described in this dissertation was focused on broadly characterizing two mouse models of inflammatory bowel disease (IBD) with emphasis on the role that genetic background plays in the development of inflammation. Differential susceptibility to experimentally-induced intestinal inflammation among various inbred mouse strains is well documented but is often not a consideration for researchers when choosing a model to recapitulate human disease. We utilized the opposing response of two strains of mice (C57BL/6 and BALB/c) to two separate chemically-induced colitis models (DSS and TNBS) to: (1) investigate the effect of genetic background on intestinal barrier function and (2) perform a genetic analysis to identify QTL regions that influence the inflammatory response in the susceptible and resistant strains for each model. We found that intestinal permeability is significantly and persistently increased in the DSS but not the TNBS model. Data from CB6F1/J mice generated from a cross between BALB/c and C57BL/6 parents suggests the BALB/c genome acts dominantly over the C57BL/6 genome in both models as the F1 mice had inflammatory responses that clustered with those of BALB/c mice. Furthermore, we were able to identify several suggestive QTL that were exclusive to each model.

Taken together, these results indicate that these models are not interchangeable, and that the final pathway of inflammation likely arises from distinct defects within each model. However, elucidation of the specific mechanisms governing inflammation and identification of genetic variants that influence susceptibility remain to be uncovered. Of additional importance is the role that resident bacteria play in the development and progression of colitis. Investigation of microbial community structure in susceptible and resistant strains of mice under each model would be instrumental for describing host-microbe interactions that may either severe

predisposing or protective functions during the inflammatory response. Collectively, data from experiments previously discussed coupled with the future work described below will be contribute to our overall understanding of the fundamental mechanisms involved in IBD pathogenesis.

Future Directions/Follow-up Studies

Microbiome Analysis

Background

The structure and function of the vertebrate intestinal tract, development of innate and adaptive immune system responses, and energy metabolism have long been influenced by the co-evolution of bacterial species and their host organisms (1). Recent exploration of the gut microbiome and its implications on human health have been made possible by advances in nucleic acid sequencing technologies and the widespread availability of bioinformatic tools. Changes in the composition of the gut microbiome have shown to be correlated with several conditions including inflammatory bowel disease (IBD), colorectal cancer (CRC), non-alcoholic fatty liver disease, rheumatoid arthritis, and obesity (2). Elucidation of the fundamental principles underlying the complex interactions between microbial communities, environmental factors, and host genetics presents an area of great interest for improving diagnostic and treatment options for diseases of the gut.

The importance of intestinal bacteria in the pathogenesis of IBD is well documented with numerous observations to support that disease results partly from uncontrolled interactions between commensal bacteria and the host immune system (2). Treatment with antibiotics is not typical but has been shown to be beneficial for acute flares and maintenance of remission in IBD patients (3-5). Specifically, the broad-spectrum antibiotics metronidazole (3,6) and ciprofloxacin

(3,7) appear to be as effective as more conventional therapies for ameliorating symptoms of Crohn's disease (CD), one of the major conditions of IBD. Furthermore, exposure to antibiotics in early childhood has been associated with an increased risk for developing CD later in life (8). In addition, the presence of an increased bacterial load in the terminal ileum of patients after ileocecal resection may be associated with postoperative relapse of inflammatory symptoms (9). Fecal stream diversion has also been demonstrated to be efficacious in reducing the characteristic inflammation associated with CD after ileal resection (10,11). Moreover, the composition of gut microbiome populations in patients affected by CD and ulcerative colitis (UC), the second major IBD condition, appear to cluster by disease type and depart from the normal structure present in the digestive tract of unaffected individuals. Significantly reduced bacterial diversity with increased proportions of Actinobacteria and Proteobacteria has been noted in twins that are discordant for UC (12). Additionally, CD patients may present with increased representation of Proteobacteria and *Enterococcus faecium* (13).

Intestinal bacteria also play a significant role in the induction and maintenance of colitis in a variety of mouse models of IBD. Spontaneous colitis develops in interleukin (IL)-10, IL2, and T-cell receptor knockout (KO) mice when animals are maintained under specific pathogen free (SPF) conditions (14-16). However, colitis can be attenuated or eliminated when these mice are reared under germ-free conditions (17) Specific bacteria of the Enterobacteriaceae family (*Proteus mirabilis* and *Klebsiella pneumoniae*) are correlated with colitis and altered barrier function in the Tbet^{-/-} x Rag2^{-/-} UC (TRUC) mouse model (18). Results gathered from animal models of IBD support that pathogenesis is in part due to abnormal immune responses to commensal bacteria that normally colonize the gut.

Significant associations between variation in the genome of host organisms and variation in the composition of their gut microbiome has been observed in both humans (19,20) and mice (21) highlighting the influence of genetic background on the presence of particular bacterial components of the gut. Fingerprinting-based comparisons of fecal samples from both monozygotic (MZ) and dizygotic (DZ) twin pairs have shown that MZ twins have a more similar population of intestinal bacteria than do DZ twins (19,20). Additionally, transplantation of fecal material from a single mouse donor into germ-free mice from three inbred strains (C57BL/10, C3H and BALB/c) resulted in microbiomes that were dissimilar from each other (21). Bacteria that colonized the intestines of C57BL/10 mice were distinctly different from bacteria found in the intestines of C3H and BALB/c mice, which more closely resembled the bacterial composition of the donor mouse (21). These results further illustrate the effect of the host genome on the establishment of an intestinal bacterial profile.

In an effort to add to the growing body of evidence supporting the impact of the intestinal bacteria on human health, we plan to conduct 16S phylogenetic analysis to characterize the gut microbiome in our two parental strains of mice (BALB/c and C57BL/6) under the two models of colitis (DSS and TNBS). Fecal samples were collected from untreated and treated mice at the time of necropsy (chapter 2). Samples from DSS treated mice will be evaluated at day 8 which corresponds to the most significant loss of body weight in susceptible C57BL/6 mice. Samples from TNBS treated mice will be evaluated at day 3 which corresponds to the most significant loss of body weight and highest disease activity index (DAI) score for susceptible BALB/c mice. In addition, samples were also collected from F1 (CB6F1/J) animals at the same timepoints for each model. All samples from treated animals will be compared to samples collected from untreated mice to determine how each chemical alters the microbiome in each strain.

Materials and Proposed Methods

DNA extraction

Fecal DNA will be isolated from 1 fecal pellet using the Qiagen MagAttract Power Soil DNA extraction kit. Samples will be quantified via Qubit 2.0 dsDNA quantification assay and normalized.

Sequencing and Analysis

Sequencing libraries will be prepared following Illumina's 16S Metagenomic Sequencing Library Preparation protocol targeting the V3-V4 variable region. Libraries will be pooled and sequenced on the Illumina MiSeq using either v2 2x250 or v3 2x300 sequencing run. 16S ribosomal phylogenetic analysis will be performed using 16S Metagenomics software (Illumina).

Potential Implications

We hope to identify bacterial orders and species associated with disease severity during experimentally-induced colitis. Identification of bacteria that are correlated with increased susceptibility or resistance to developing inflammation could prove useful for prognosis and treatment of human IBD. Reduced numbers of the phyla Firmicutes and Bacteroidetes, and increased numbers of Actinobacteria and Proteobacteria have been observed in patients with IBD (22-24). However, it remains unclear as to whether these differences are causative or a consequence of the development of IBD. Comparisons of the intestinal microbiome before and after experimentally-induced inflammation could be informative for delineating cause from consequence.

Because the intestinal microbiome of patients with IBD appears to have reduced diversity compared with that of healthy subjects, there has been increasing focus on the therapeutic potential of fecal microbiota transplants (FMT) to ameliorate symptoms of inflammation (25). A

meta-analysis of FMT for UC patients found that 63% of patients with UC entered remission, 76% were able to stop taking medications for IBD, and 76% experienced a reduction in gastrointestinal (GI) symptoms (26). Results from our microbiome analysis could potentially identify bacterial species that are associated with resistance to inflammation. Healthy individuals harboring these bacteria in their guts could then be selected for FMT for the treatment of IBD.

Probiotics have also emerged as a promising new alternative for the prevention and treatment of gastrointestinal inflammatory diseases. Some probiotic mixtures have been successful in reducing disease severity in patients suffering from UC (27). However, the use of probiotics has been less efficacious when applied to patients affected by CD (28). Animal models have also been valuable in elucidating the effectiveness of probiotics on reducing inflammatory responses. Notably, five strains of bacteria were identified as being highly protective in both DSS and TNBS-induced colitis (29). The protective effect of these strains was attributed to their ability to strengthen the intestinal barrier and to limit epithelial injury (29). Mice that were pretreated with these bacteria did not experience the decreased expression of tight junction proteins (ZO-1, OCLN, and CLDN5) that is typical in chemically-induced colitis models(29). Furthermore, they showed significant improvements in gut permeability as measured by decreased passage of FITC-dextran from the intestine into the blood (29). Species associated with resistant phenotypes from our microbiome analysis could be selected for inclusion in probiotic mixtures to protect against the development of IBD or to help alleviate symptoms of UC or CD.

Lastly, quantitative genetic approaches have recently been used to explain the influence of host genetics on compositional features of the gut microbiome. A study utilizing an advanced intercross line mapping population generated 16S rRNA gene sequences from 645 mice and was

able to identify 18 quantitative trait loci (QTL) that contributed to microbiota composition (30). A core of measurable microbiota (CMM) consisting of 64 conserved taxonomic groups was also identified (30). QTL analysis using the well characterized BXD (C57BL/6 x DBA/2) mouse recombinant inbred panel was able to uncover several candidate genes that potentially influence gut microbial communities (31). A QTL region on chromosome 4 appeared to modulate the predominant BXD gut phyla populations, Bacteroidetes and Firmicutes (31). Another QTL chromosome 15 seemed to modulate the bacterial family Rikenellaceae and harbors the *Tgfb3* gene which produces a cytokine involved in regulating barrier function of the intestine and tolerance to commensal bacteria (31). We collected fecal samples from our F2 (F2CB) mapping population (chapter 3) for both the DSS and TNBS models. These samples could be used to identify QTL influencing any differences in microbial composition found in the analysis of 16S data from the parental strains (BALB/c and C57BL/6) described above. This combined approach could be instrumental in identifying bacterial species and host genetic variants that affect disease severity in human IBD.

Intestinal Permeability Follow-up

In chapter 2, we described the effect of genetic background on intestinal permeability. There are several follow-up experiments that may be useful in describing the underlying differences in permeability found in the two chemical models of inflammation. First, measurements of baseline permeability were limited to samples from the distal colon. However, *in vivo* quantification of permeability via FITC-Dextran flux was not restricted to a particular region of the GI tract but instead surveyed the leakiness of the entire length of intestine. Additional Ussing chamber runs on tissues from various areas of the GI tract (dudodenum, jejunum, ileum, and proximal colon) might be informative in capturing any innate variation that

might be present in gut permeability between BALB/c and C57BL/6 mice. This may be of particular importance for the TNBS model, which is supposed to be representative of human CD that preferentially affects the ileum and colon but may also affect other areas of the intestine (32).

We showed that barrier function in susceptible C57BL/6 mice was significantly and persistently perturbed in the DSS model; however, no significant variation in barrier function was found in susceptible BALB/c mice in the TNBS model. This may be in part due to the time frame at which permeability was evaluated in TNBS treated mice. In the TNBS model, ethanol (EtOH) is used to disrupt the epithelial barrier allowing TNBS to haptenize intestinal proteins that stimulate the inflammatory response. A study in rats found that brief (30-45 seconds) exposure of the intestinal epithelium to EtOH destroyed more than 95% of the superficial epithelial cells and exposed the basal lamina propria (33). After 1 hour, greater than 90% of the exposed lamina had been covered by migrating mucosal cells in an effort to restore the damaged barrier (33). Perhaps BALB/c mice experience impaired barrier repair in comparison to C57BL/6 mice; however, 3 days post-TNBS administration may be too late to capture this difference since the barrier has likely been repaired in both strains. The inflammatory response is observable as soon as 1-day post-TNBS administration in susceptible BALB/c mice. Evaluation of intestinal permeability at this time point may be more informative in detecting differences in barrier repair between the two strains.

QTL Mapping Follow-up

In chapter 3, we utilized the F2CB mapping population in an effort to identify QTL affecting disease severity in DSS and TNBS-induced colitis. We were unable to successfully

detect statistically significant QTL, but implementation of several additional and complementary experiments was discussed. Here, I describe a follow-up experiment not previously mentioned.

The potential effect of maternal factors has previously been shown in a similar study to map QTL in a bacterially-induced model of IBD (34). A distinct difference between the response of A/J and C57BL/6 mouse strains to infection with the bacterium *Helicobacter hepaticus* is well-documented (35-37) and served as the basis for QTL detection (34). Susceptible A/J mice developed overexpression of proinflammatory cytokines followed by chronic cecal inflammation, whereas infected C57BL/6 mice fail to develop cecal inflammation or increased cytokine expression. Cecal expression of IL-12/23p4 was identified as biomarker for disease severity (36,38-40) and used to map QTL in a F2 population generated from F1 parents from reciprocal crosses of A/J and C57BL/6 mice, termed AB6 and B6A (34). Biomarker expression was significantly lower than A/J mice but not significantly different from in C57BL/6 mice for the AB6 F1 mice (34). However, expression levels in B6A F1 mice were significantly lower than A/J controls and significantly higher than C57BL/6 controls (34). These results were speculated to be a consequence of either paternally imprinted genes or the maternal environment.

Our CB6F1/J hybrid mice were the offspring of a cross between BALB/c females and C57BL/6 males. In order to account for the possible effects described above, another population of F1 mice could be created from a reciprocal cross of C57BL/6 females and BALB/c males. The four possible crosses from a combination of the two F1 populations could then be used to generate the F2 mapping population for QTL analysis. F2 mice resulting from the proposed breeding would then be able to account for differences in phenotype due to parental pairing or maternal effects.

Conclusions

We have demonstrated the effect of genetic background on the development of experimentally-induced colitis in two separate models of human IBD. We have attempted to characterize these models in terms of intestinal barrier modulation, as well as, the identification of genetic variants that may influence disease severity in susceptible and resistant strains of mice. Several studies conducted by other groups have also evaluated the effect of genetic background on the development of intestinal inflammation; however, those studies were limited to evaluation in only one experimental model. We utilized a novel comparative approach to investigate the mechanisms that govern inflammation in two distinct models of IBD.

The opposing responses of BALB/c and C57BL/6 mice to DSS and TNBS-induced colitis, respectively, presented a unique opportunity to explore the underlying processes of inflammation on the same genetic backgrounds under two separate experimental conditions. The significance of this work lies in its multifaceted approach for characterizing the inflammatory responses in these commonly used animal models of disease. Human UC and CD are distinct diseases that present with both unique and shared pathology, and the same holds true for DSS and TNBS-induced colitis. As such, understanding both the similarities and differences involved in the pathogenesis of these models is of the utmost importance for researchers when determining which models are best suited to answer their experimental questions. The results of a study are only as good as the experimental design used to obtain them. Therefore, a more complete understanding of animal models that are used to recapitulate human disease is essential for maintaining the validity of experimental results and conclusions. It is our hope that the research presented here combined with proposed future experiments and follow-up studies will

be a valuable resource for other scientist who wish to investigate the fundamental mechanisms involved in IBD pathogenesis.

References

- (1) Knight R, Gordon JI, Lozupone CA, Ley RE, Hamady M. Worlds within worlds: evolution of the vertebrate gut microbiota. *Nature Reviews Microbiology* 2008;6(10):776-788.
- (2) Cho I, Blaser MJ. The human microbiome: at the interface of health and disease. *Nature reviews. Genetics* 2012 Mar 13;13(4):260-270.
- (3) Prantera C, Zannoni F, Scribano ML, Berto E, Andreoli A, Kohn A, et al. An antibiotic regimen for the treatment of active Crohn's disease: a randomized, controlled clinical trial of metronidazole plus ciprofloxacin. *The American journal of gastroenterology* 1996;91(2):328-332.
- (4) Rutgeerts P, Hiele M, Geboes K, Peeters M, Penninckx F, Aerts R, et al. Controlled trial of metronidazole treatment for prevention of crohn's recurrence after ileal resection. *Gastroenterology* 1995;108(6):1617-1621.
- (5) Arnold GL, Beaves MR, Pryjdun VO, Mook WJ. Preliminary Study of Ciprofloxacin in Active Crohn's Disease. *Inflammatory bowel diseases* 2002;8(1):10-15.
- (6) Ursing B, Alm T, Bárány F, Bergelin I, Ganrot-Norlin K, Hoevens J, et al. A comparative study of metronidazole and sulfasalazine for active Crohn's disease: the cooperative Crohn's disease study in Sweden. II. Result. *Gastroenterology* 1982;83(3):550-562.
- (7) Colombel J, Lémann M, Cassagnou M, Bouhnik Y, Duclos B, Dupas J, et al. A controlled trial comparing ciprofloxacin with mesalazine for the treatment of active Crohn's disease. *American Journal of Gastroenterology* 1999;94(3):674-678.
- (8) Hviid A, Svanström H, Frisch M. Antibiotic use and inflammatory bowel diseases in childhood. *Gut* 2011;60(1):49-54.
- (9) Neut C, Bulois P, Desreumaux P, Membré J, Lederman E, Gambiez L, et al. Changes in the bacterial flora of the neoterminal ileum after ileocolonic resection for Crohn's disease. *American Journal of Gastroenterology* 2002;97(4):939-946.
- (10) Harper PH, Truelove SC, Lee EC, Kettlewell MG, Jewell DP. Split ileostomy and ileocolostomy for Crohn's disease of the colon and ulcerative colitis: a 20year survey. *Gut* 1983;24(2):106-113.
- (11) Rutgeerts P, Peeters M, Hiele M, Vantrappen G, Pennincx F, Aerts R, et al. Effect of faecal stream diversion on recurrence of Crohn's disease in the neoterminal ileum. *The Lancet* 1991;338(8770):771-774.
- (12) Lepage P, Häsler R, Spehlmann ME, Rehman A, Zvirbliene A, Begun AI, Ott S, Kupcinskas L, Doré J, Raedler A, Schreiber S. Twin Study Indicates Loss of Interaction Between

Microbiota and Mucosa of Patients with Ulcerative Colitis. *Gastroenterology* 2011;141(1):227-236.

- (13) Mondot S, Kang S, Furet JP, Aguirre de Carcer D, McSweeney C, Morrison M, et al. Highlighting new phylogenetic specificities of Crohn's disease microbiota. *Inflammatory bowel diseases* 2011;17(1):185-192.
- (14) Kühn R, Löhler J, Rennick D, Rajewsky K, Müller W. Interleukin-10-deficient mice develop chronic enterocolitis. *Cell* 1993;75(2):263-274.
- (15) Sadlack B, Merz H, Schorle H, Schimpl A, Feller AC, Horak I. Ulcerative colitis-like disease in mice with a disrupted interleukin-2 gene. *Cell* 1993;75(2):253-261.
- (16) Mombaerts P, Mizoguchi E, Grusby MJ, Glimcher LH, Bhan AK, Tonegawa S. Spontaneous development of inflammatory bowel disease in T cell receptor mutant mice. *Cell* 1993;75(2):275-282.
- (17) Dianda L, Hanby AM, Wright NA, Sebesteny A, Hayday AC, Owen MJ. T cell receptor-alpha beta-deficient mice fail to develop colitis in the absence of a microbial environment. *American Journal of Pathology* 1997;150(1):91-97.
- (18) Garrett WS, Gallini CA, Yatsunencko T, Michaud M, DuBois A, Delaney ML, et al. Enterobacteriaceae Act in Concert with the Gut Microbiota to Induce Spontaneous and Maternally Transmitted Colitis. *Cell Host & Microbe* 2010;8(3):292-300.
- (19) Stewart JA, Chadwick VS, Murray A. Investigations into the influence of host genetics on the predominant eubacteria in the faecal microflora of children. *Journal of Medical Microbiology* 2005;54(12):1239-1242.
- (20) Zoetendal EG, Akkermans ADL, Akkermans-van Vliet WM, J. de Visser AGM, de Vos WM. The Host Genotype Affects the Bacterial Community in the Human Gastrointestinal Tract. *Microbial Ecology in Health and Disease* 2001;13(3):129-134.
- (21) Loh G, Brodziak F, Blaut M. The Toll-like receptors TLR2 and TLR4 do not affect the intestinal microbiota composition in mice. *Environmental microbiology* 2008;10(3):709-715.
- (22) Qin J, Li R, Raes J, Arumugam M, Tims S, Vos d, W.M, et al. A human gut microbial gene catalogue established by metagenomic sequencing. *Nature* 2010;464(7285):59-65.
- (23) Frank DN, Robertson CE, Hamm CM, Kpadeh Z, Zhang T, Chen H, et al. Disease phenotype and genotype are associated with shifts in intestinal-associated microbiota in inflammatory bowel diseases. *Inflammatory bowel diseases* 2011;17(1):179-184.

- (24) Ott SJ, Musfeldt M, Wenderoth DF, Hampe J, Brant O, Fölsch UR, et al. Reduction in diversity of the colonic mucosa associated bacterial microflora in patients with active inflammatory bowel disease. *Gut* 2004;53(5):685-693.
- (25) Smits LP, Bouter KEC, de Vos WM, Borody TJ, Nieuwdorp M. Therapeutic Potential of Fecal Microbiota Transplantation. *Gastroenterology* 2013;145(5):946-953.
- (26) Anderson JL, Edney RJ, Whelan K. Systematic review: faecal microbiota transplantation in the management of inflammatory bowel disease. *Alimentary Pharmacology & Therapeutics* 2012;36(6):503-516.
- (27) Sáez-Lara MJ, Gómez Llorente C, Plaza-Díaz J, Gil Á. The Role of Probiotic Lactic Acid Bacteria and Bifidobacteria in the Prevention and Treatment of Inflammatory Bowel Disease and Other Related Diseases: A Systematic Review of Randomized Human Clinical Trials. 2015.
- (28) Lichtenstein L, Avni-Biron I, Ben-Bassat O. Probiotics and prebiotics in Crohn's disease therapies. *Best Practice & Research: Clinical Gastroenterology* 2016;30(1):81-88.
- (29) Zaylaa M, Al Kassaa I, Alard J, Peucelle V, Boutillier D, Desramaut J, et al. Probiotics in IBD: Combining in vitro and in vivo models for selecting strains with both anti-inflammatory potential as well as a capacity to restore the gut epithelial barrier. *Journal of Functional Foods* 2018; 47:304-315.
- (30) Benson AK, Kelly SA, Legge R, Ma F, Low SJ, Kim J, et al. Individuality in gut microbiota composition is a complex polygenic trait shaped by multiple environmental and host genetic factors. *Proceedings of the National Academy of Sciences of the United States of America* 2010;107(44):18933-18938.
- (31) McKnite AM, Lu L, Williams E, Bastiaansen JWM. Murine Gut Microbiota Is Defined by Host Genetics and Modulates Variation of Metabolic Traits. *PLoS One* 2012;7(6): e39191.
- (32) Mak WY, Hart AL, Ng SC. Crohn's disease. *Medicine* 2019;47(6):377-387.
- (33) Lacy ER, Ito S. Rapid epithelial restitution of the rat gastric mucosa after ethanol injury. *Laboratory investigation; a journal of technical methods and pathology* 1984;51(5):573-583.
- (34) Hillhouse A, Myles M, Taylor J, Bryda E, Franklin C. Quantitative trait loci in a bacterially induced model of inflammatory bowel disease. *Mamm Genome* 2011;22(9):544-555.
- (35) J G Fox, L Yan, B Shames, J Campbell, J C Murphy, X Li. Persistent hepatitis and enterocolitis in germfree mice infected with *Helicobacter hepaticus*. *Infection and Immunity* 1996 Sep 1;64(9):3673-3681.

- (36) Myles MH, Dieckgraefe BK, Criley JM, Franklin CL. Characterization of cecal gene expression in a differentially susceptible mouse model of bacterial-induced inflammatory bowel disease. *Inflammatory bowel diseases* 2007;13(7):822-836.
- (37) Whary MT, Morgan TJ, Dangler CA, Gaudes KJ, Taylor NS, Fox JG. Chronic Active Hepatitis Induced by *Helicobacter hepaticus* in the A/JCr Mouse Is Associated with a Th1 Cell-Mediated Immune Response. *Infection and Immunity* 1998;66(7):3142-3148.
- (38) Kullberg MC, Rothfuchs AG, Jankovic D, Caspar P, Wynn TA, Gorelick PL, et al. *Helicobacter hepaticus*-Induced Colitis in Interleukin-10-Deficient Mice: Cytokine Requirements for the Induction and Maintenance of Intestinal Inflammation. *Infection and Immunity* 2001;69(7):4232-4241.
- (39) Neurath MF. Antibodies to interleukin 12 abrogate established experimental colitis in mice. *Journal of Experimental Medicine* 1995;182(5):1281-1290.
- (40) Peyrin-Biroulet L, Desreumaux P, Sandborn WJ, Colombel J. Crohn's disease: beyond antagonists of tumour necrosis factor. *Lancet* 2008;372(9632):67-81.